

*This article was originally submitted as one contribution to a prospective Focus Issue tentatively entitled "What Have We Learned from One-dimensional Maps?" Consequently, the article focuses more on the authors' own results than would an appropriately complete survey of the statistical properties of 1D maps. However, in view of the postponement of this Focus Issue, in order to avoid undue delay in the publication of these results, the editors have decided to publish the article in its present form, rather than asking the authors to redo the article entirely.*

## Statistical properties of chaos demonstrated in a class of one-dimensional maps

András Csordás

*Research Institute for Solid State Physics of the Hungarian Academy of Sciences, P. O. Box 49,  
H-1525 Budapest, Hungary*

Géza Györgyi

*Institute for Theoretical Physics, Eötvös University, Puskin u. 5-7, H-1088 Budapest, Hungary*

Péter Szépfalusy

*Institute for Solid State Physics, Eötvös University, Múzeum krt. 6-8, H-1088 Budapest, Hungary  
and Research Institute for Solid State Physics of the Hungarian Academy of Sciences, P. O. Box 49,  
H-1525 Budapest, Hungary*

Tamás Tél

*Institute for Theoretical Physics, Eötvös University, Puskin u. 5-7, H-1088 Budapest, Hungary*

(Received 4 February 1992; accepted for publication 16 November 1992)

One-dimensional maps with complete grammar are investigated in both permanent and transient chaotic cases. The discussion focuses on statistical characteristics such as Lyapunov exponent, generalized entropies and dimensions, free energies, and their finite size corrections. Our approach is based on the eigenvalue problem of generalized Frobenius–Perron operators, which are treated numerically as well as by perturbative and other analytical methods. The examples include the universal chaos function relevant near the period doubling threshold. Special emphasis is put on the entropies and their decay rates because of their invariance under the most general class of coordinate changes. Phase-transition-like phenomena at the border state of chaos due to intermittency and super instability are presented.

### I. INTRODUCTION AND SUMMARY

The most well-known role one-dimensional (hereafter 1D) maps played in the development of the theory of chaotic phenomena is connected with the different routes to chaos and the related metric universality.<sup>1</sup> In higher-dimensional dissipative systems, scenarios like period doubling, the quasiperiodic route, and intermittency were found to exhibit scaling properties which could be led back to those of certain 1D maps near the threshold to chaos. Furthermore, substantial research was expended on 1D chaos in its developed state and a richness of statistical properties has been revealed, which constitute the main concern of this paper. The significance of 1D maps is underscored by the fact that new ideas about general chaotic systems are often tried out and exemplified on 1D maps in the literature. A further motivation for studying 1D maps is that many higher-dimensional systems in the limit of strong dissipation approximately reduce to 1D dynamics. This is supported by a variety of experimental evidences.<sup>2</sup> Near the threshold to chaos on its chaotic side the effective dissipation can be that strong that eventually a fully chaotic 1D map with universal characteristics emerges on small length and long time scales. Thus a link between the transition to chaos and the fully developed chaos can be established.

We shall concentrate on multifractal-like statistical characteristics providing a detailed description of certain

chaotic features. Scaling of a uniform covering of the attractor is characterized by the fractal dimension. The natural invariant measure on the attractor generated by the dynamics might have very rich local scaling properties.<sup>3</sup> To describe them, besides the fractal dimension, a full spectrum of dimensionlike quantities is required. Measures with nontrivial spectrum of dimensions are termed multifractals.<sup>4,5</sup> Although chaotic attractors of 1D maps generally do not exhibit nontrivial fractal properties, their dynamical characteristics like the path probability distribution of the symbolic codes do. Symbolic codes are coarse grained representations of trajectories, such that the phase space is divided into finite cells and a discrete valued symbol is associated with each of them. Following the trajectory, the information in which order the cells are visited is contained in the sequence of symbolic codes. The probabilities of allowed sequences in the space of the symbolic codes taken with respect to the natural measure define a special multifractal called dynamical multifractal.<sup>6</sup> Such dynamical multifractals are described by the spectrum of generalized entropies.<sup>7,8</sup> Similarly, the fluctuation of finite-time Lyapunov exponents<sup>9,10</sup> defines another spectrum connected with the inherent instability of the chaotic motion.

Different types of thermodynamical formalisms<sup>11–13</sup> provide a natural framework for the description of the above-mentioned phenomena and statistical characteris-

tics. Within these statistical descriptions relevant characteristics of chaos can be obtained in analogy with traditional equilibrium statistical mechanics. In this paper special emphasis will be put on the free energy equivalent to the generalized entropies, for they are invariant under a most general class of coordinate changes which may also contain singularities. We shall also be interested in how rapidly quantities derived from symbol sequences of finite length approach the entropies, i.e., in finite-size corrections to the limiting values. In contrast to other dynamical multifractal spectra where nonanalytic behavior—sometimes called phase transition<sup>14–19</sup>—is not uncommon, in the entropy spectrum they turn out to be rather rare and show up at the border states of chaos.<sup>20–23</sup> To understand such situations we recall that unstable periodic orbits are dense on the invariant set on which the chaotic motion takes place. Generally, the Lyapunov exponents for all the unstable orbits are bounded from below and above by two positive finite numbers. Situations, when for a chaotic system one of the bounds is infinity or zero, or when the given system can be transformed into such a system, will be called border states of chaos. (In higher-dimensional systems one should consider in this context the largest Lyapunov exponent.)

In contrast to the above cases where chaos is permanent, many dynamical systems exhibit chaotic behavior in their transients.<sup>24</sup> Signals produced by them look chaotic for a certain time before reaching stationarity, which can be chaos and regular motion alike. In these cases, invariant objects exist in phase space, different from attractors, called chaotic repellers, which are Cantor sets of measure zero. With the exception of these points all initial conditions lead to trajectories which eventually leave the interval of interest. Trajectories starting close to a repeller produce long, transiently chaotic signals. The multifractal properties of the invariant set play an important role in determining the dynamical properties of transient chaotic systems.

We restrict our attention to *complete* (permanently or transiently) chaotic maps on the interval. To understand its definition let us consider piecewise monotonic maps defined on an interval  $I$ . Consider, furthermore, the subintervals which are the preimages of the monotonic branches and introduce a symbolic dynamics by attaching different symbols to each of them. We say the map is complete if all the possible symbolic code combinations are allowed by the dynamics on the invariant set. This is the case only if the inverses of the monotonic branches are defined on the entire interval  $I$ . Then denoting by  $m$  the number of monotonic branches, the topological entropy is equal to  $\ln m$ . To be specific, we choose complete chaotic maps with one increasing and one decreasing monotonic branch with  $\ln 2$  as the topological entropy. With this restriction of considering complete maps only, the complications caused by nontrivial grammatical rules, i.e., by the exclusion of certain symbol sequences, are absent and a presentation that focuses on the essential points becomes possible. The discussion of properties which are connected with pruning of the grammar<sup>25</sup> is thus beyond the scope of the paper.

It is an organizing principle of our description that all

the characteristics exhibiting invariance properties are related to eigenvalues of certain generalized Frobenius–Perron operators.<sup>26–28,22</sup> The operator formalism provides us with a practical tool for computing characteristics of chaos with high accuracy.

This paper is organized as follows. Section II is devoted to complete maps generating permanent chaos. After a brief summary of the elements of the statistical description (natural measure, correlation decay), a general classification of such maps is given which will be used throughout the paper. It is shown that all complete maps can be reached by means of a conjugation and a transformation transverse to it. Next, through the finite size correction to the Kolmogorov–Sinai entropy the entropy decay rate is introduced as a new dynamical characteristics. A central object of the theory is the Frobenius–Perron equation describing the time evolution of probability densities on the attractor. For maps lying in some sense close to exactly solvable ones, analytic results can be obtained by means of a perturbation expansion of the Frobenius–Perron equation. This method is then outlined with technical details relegated to Appendix A. Illustrative results are given for maps related to the tent map via the transformation transverse to conjugation, provided the transformation deviates little from the identity but otherwise it can be of arbitrary form. As another application we present properties of the universal chaos function which is relevant near the period doubling threshold of chaos. In Sec. III complete maps generating transient chaos are investigated. The notion of the natural measure and of the related conditionally invariant measure is discussed first. The density of these measures are shown to be obtainable from extensions of the classical Frobenius–Perron equation. Next, fractal properties of the strange set are investigated and brought in relation with other generalizations of the Frobenius–Perron equation. As an example, it is shown how the dimensions of the universal period doubling attractor can be determined by considering it as a repeller of an auxiliary map.

The thermodynamic formalism of both permanently and transiently chaotic maps of complete type is summarized in Sec. IV. It is shown how entropies, the free energy associated with the lengths of subintervals, the generalized Lyapunov exponents, and dimensions can be obtained from the growth rate of different partition sums. They can be expressed via the largest eigenvalue of different generalized Frobenius–Perron operators. The approach to the asymptotic limit is also discussed which is related to the largest and second largest eigenvalues of suitable operators. Results obtained from the perturbation expansion of the spectrum of the generalized Frobenius–Perron operator are given in terms of a general transverse transformation for classes of complete maps. Finally, singular behaviors, so-called phase transitions, in the characteristics are investigated with special emphasis on the entropies. It is shown that entropies exhibit phase transitions in intermittent and in extremely unstable cases, both representing border states of the chaotic phase.

In the outlook we summarize those features of chaos generated by complete 1D maps which remain valid in

more complicated 1D cases and in higher-dimensional systems, too. It is pointed out that 1D maps also show up in the statistical mechanics of 1D lattices which can be studied by means of the methods discussed here. This is illustrated on the example of the random field Ising chain in Appendix B.

## II. FULLY DEVELOPED CHAOTIC MAPS

The study of chaotic iterations is based on the fact that trajectories are asymptotically distributed according to a unique probability density function, the density of the natural measure. The evaluation of characteristics of chaos are led back to manageable averages, or which are so at least in some asymptotic sense. A simple type of such maps are the fully developed chaotic ones, which fill an interval with most chaotic iterations. Such maps emerge in parameter controlled maps not only as the final stage of the evolution of the attractor,<sup>3</sup> but also at the band merging<sup>29</sup> and crisis<sup>30</sup> points, if appropriate iterates of the original map are considered. In particular, the universal chaos function<sup>31</sup> belongs to this category, too.

### A. Elements of the statistical description

We investigate chaotic iterations generated by single humped 1D maps of the interval  $I=[0,1]$

$$x_{n+1}=f(x_n). \quad (1)$$

Maps generating fully developed chaos (FDC)<sup>32</sup> are specified by the properties that the function  $f(x)$  is piecewise differentiable, it is two-to-one on the interval  $I$ , it increases in  $[0,\hat{x}]$  and decreases in  $[\hat{x},1]$  monotonically,  $f(0)=f(1)=0$  and  $f(\hat{x})=1$  (see Fig. 1). It is assumed that the map does not have any stable periodic orbits in  $I$ , rather it generates ergodic trajectories for almost all initial conditions within the interval. The definition further requires that there exists a unique invariant ergodic measure  $\mu$ , which is absolutely continuous with respect to the Lebesgue measure, and thus there is a probability density function  $P(x)$ . Only such measure, called the natural measure, will be considered throughout this section.

Ergodicity implies that the time average of a function  $A(x)$  can be represented by a weighted average over the interval

$$\lim_{N \rightarrow \infty} \frac{1}{N} \sum_{n=0}^N A(x_n) = \int_I A(x)P(x)dx. \quad (2)$$

The above relation should hold for the composed function  $A(f(x))$  as well, hence,

$$\int_I A(x)P(x)dx = \int_I A(f(x))P(x)dx. \quad (3)$$

Since that relation is valid for a general  $A(x)$ , we can write

$$P(x) = \int_I \delta(x-f(y))P(y)dy \equiv \hat{H}P(x), \quad (4)$$

which defines the linear operator  $\hat{H}$ . The integral operator can also be written in the form

$$\hat{H}P(x') = \sum_{x \in f^{-1}(x')} \frac{P(x)}{|f'(x)|}, \quad (5)$$

where  $f^{-1}(x')$  stands for the set of the preimages  $x$  of  $x'$ . For FDC maps each  $x' < 1$  has two preimages. Equation (4) is often called the Frobenius–Perron equation and the operator  $\hat{H}$  bears the same name. Note that for FDC maps with quadratic maximum  $P(x)$  has singularities of order  $-1/2$  at the endpoints of the interval  $I$ . Acting on a general probability density the Frobenius–Perron operator defines the recursion

$$P_{n+1} = \hat{H}P_n(x) \quad (6)$$

which is the time evolution of the distribution function if the points  $x$  are evolved by the map (1).

The invariant density allows us to write the average characteristics of the iteration in integral form. The Lyapunov exponent is measuring the average divergence rate of nearby trajectories

$$L \equiv \lim_{N \rightarrow \infty} \frac{1}{N} \sum_{n=0}^N \ln \left| \frac{dx_{n+1}}{dx_n} \right| = \int_I P(x) \ln |f'(x)| dx \quad (7)$$

( $'$  denotes derivative throughout this paper). Besides, correlation functions characterize the decay of memory along the iteration. The correlation of functions  $A(x)$  and  $B(x)$  is defined by

$$C_{AB}(n) = \int_I P(x)A(x)B(f^{(n)}(x))dx - \int_I P(x)A(x)dx \int_I P(x)B(x)dx. \quad (8)$$

For chaotic iterations the correlation function is expected to have a decaying component. It is easy to show, that the  $n$  dependence of the correlation function can be traced back to  $n$  applications of the Frobenius–Perron operator, since the first term on the right-hand side of (8) equals

$$\int_I B(x)\hat{H}^n[A(x)P(x)]dx. \quad (9)$$

The time behavior of the correlation function can thus be determined by investigating the spectral properties of  $\hat{H}$ . The existence of the unique invariant density  $P(x)$  implies that the eigenvalue largest in modulus is  $\lambda_0=1$ . Assume, that there is a second largest real eigenvalue  $|\lambda_1| < 1$ , then one obtains that for  $n \rightarrow \infty$

$$C_{AB}(n) \propto \lambda_1^n. \quad (10)$$

It is worth defining an asymptotic correlation decay rate  $r$  via  $r = -\ln|\lambda_1|$ .

### B. Classification of FDC maps

Equivalence classes of FDC maps are defined by smooth coordinate transformations, called conjugation.<sup>33</sup> If in Eq. (1) both  $x_n$  and  $x_{n+1}$  are transformed by the same  $u(x)$  function, which is invertible and  $u(0)=0$ ,  $u(1)=1$ , then the transformed map is

$$g(x) = u(f(u^{-1}(x))). \quad (11)$$

The function  $u(x)$  must be piecewise differentiable and we will call it nonsingular if  $0 < u'(x) < \infty$ . Note that singular transformations can create or eliminate critical points, where the derivative of the map vanishes. Characteristics of chaos invariant under such transformation are of special interest, such as the Lyapunov exponent, correlation decay rate, and as we shall see it later, the generalized entropies and their decay rates.

Consider first symmetric maps, defined by  $f(x) = f(1-x)$ . In the special case when the probability density is also symmetric,  $P(x) = P(1-x)$ , we speak about *double symmetry*. The archetype for the latter family is the piecewise linear tent map having uniform invariant density

$$f_L(x) = 1 - |1 - 2x|, \quad P_L(x) = 1. \quad (12)$$

Each map  $f_D$  of double symmetry is related to the tent map by conjugation with  $u(x) = 1 - u(1-x)$ . Then for  $f_D$  the invariant measure of the interval  $[0, x]$ , i.e.,  $\int_0^x P(x) dx \equiv \mu(x)$  equals  $u(x)$ . For instance,  $u(x) = 2/\pi \arcsin \sqrt{x}$  gives the quadratic logistic map

$$f_Q(x) = 4x(1-x), \quad P_Q(x) = \frac{1}{\pi \sqrt{x(1-x)}}. \quad (13)$$

All double symmetric maps possess the maximal possible Lyapunov exponent  $L_D = \ln 2$ , and the decay rate of typical correlation functions is  $r_D = \ln 4$ .

An operation *transverse to conjugation* can also be defined<sup>34,35</sup> such that if applied to a double symmetric map it results in a symmetric map and the difference between the original and the transformed probability densities has odd symmetry. As an example, the maps obtained from the tent map  $f_L$  are implicitly defined as

$$f(x) = f_L(x) - v(f(x)), \quad P(x) = 1 + v'(x), \quad (14)$$

where  $v(x)$  is a symmetric function,  $v(x) = v(1-x)$ , with  $v(0) = 0$ . Further requirements on  $v(x)$  are provided by its connection to  $P(x)$ . As the second expression shows,  $v'(x)$  measures the deviation of the invariant density from unity and obviously cannot be less than  $-1$ . We will call (14) the transverse map for short. This is an important class of maps, because *all* FDC maps, symmetric and nonsymmetric ones alike, are conjugated to a map of the form (14).

As an example let  $v(x) = dx(1-x)$ ,  $|d| \leq 1$ , leading to the piecewise parabolic map

$$\begin{aligned} f_{PP}(x) &= (2d)^{-1} (d+1 - \sqrt{(d-1)^2 + 4d|1-2x|}), \\ P_{PP}(x) &= 1 + d(1-2x). \end{aligned} \quad (15)$$

The two extreme values for  $d$  represent qualitatively different cases. For  $d = -1$  the map has an infinite initial slope, thus the dynamics near the origin is very fast expanding. For  $d = 1$  the phenomenon of weak intermittency emerges,<sup>36,37</sup> namely,  $f'(0) = 1$ , and despite this an ergodic invariant measure still exists, see (15). It is worth emphasizing that for general  $v(x)$  the two extreme situations occur for  $v'(0) = -1$  and  $v'(0) = 1$ , respectively.

In the following we will use the fact that each FDC map is conjugate to a map for which the natural invariant measure is the Lebesgue measure. Indeed, if we use the invariant measure of the interval  $[0, x]$  of  $f$ , i.e.,  $\mu(x)$ , as conjugating function, we get

$$\tilde{f}(x) = \mu(f(\mu^{-1}(x))), \quad \tilde{\mu}(x) = x. \quad (16)$$

We will call that map the equivalent Lebesgue map of  $f(x)$ . For our purposes it will be important that  $|f'(x)| \geq 1$ . On Fig. 2 the schematic topological structure of the space of FDC maps is displayed.

### C. Symbolic dynamics, the Kolmogorov-Sinai entropy, and entropy decay

So far we introduced characteristics of the chaotic behavior of the continuous dynamical variable  $x$ , like its probability density, the Lyapunov exponent and correlation function. Further insight is gained into the complex nature of chaos by studying the coarse grained, or, symbolic dynamics.<sup>38</sup> A central quantity characterizing the latter is the Kolmogorov-Sinai (KS)<sup>39-41</sup> entropy, a positive finite value of which is often considered as a criterion for chaos.

Let us start out from the partition of  $I$  into  $I_0^{(1)} = [0, \hat{x}]$  and  $I_1^{(1)} = [\hat{x}, 1]$ . Write  $f^{-k}(I_j^{(1)})$  for the set of points mapped to  $I_j^{(1)}$  ( $j=0,1$ ) by  $k$  application of the map  $f$ . Then the subintervals of the partition in the  $n$ th generation are

$$I_i^{(n)} = I_{a_1}^{(1)} \cap f^{-1}(I_{a_2}^{(1)}) \cap \dots \cap f^{-n+1}(I_{a_n}^{(1)}), \quad (17)$$

where  $a_k$  is either 0 or 1, and  $i = \sum_{k=1}^n a_k 2^{k-1}$ . The subintervals  $\{I_i^{(n)}\}_{i=0}^{2^n-1}$  are all nonoverlapping preimages of  $I$  for FDC maps and they provide full coverage for  $I$ . Such intervals are called cylinder sets in the mathematical literature. For FDC maps the number of subintervals increase by the same integer factor 2 in subsequent generations, such hierarchy of branching is called complete. Note that there is a one-to-one correspondence between an orbit in symbol space  $a_1 \dots a_n$  and the integer  $i$ . The interval  $I_i^{(n)}$  is just the set of initial conditions which generates the symbolic orbit associated with  $i$ , so the stationary probability of the orbit  $P(a_1 \dots a_n)$  is the invariant measure of that interval, denoted here by  $\mu_i^{(n)} \equiv \mu(I_i^{(n)})$ . The partition is a generating partition.<sup>41</sup> Thus the KS entropy is given by

$$\begin{aligned} K &= \lim_{n \rightarrow \infty} K_n, \\ K_n &= -\frac{1}{n} \sum_i \mu(I_i^{(n)}) \ln \mu(I_i^{(n)}). \end{aligned} \quad (18)$$

There is another sequence of entropies through which one can directly extract a characteristic time associated with symbolic dynamics. In the general case symbolic dynamics has infinitely long memory. Thus an error is committed by truncating the memory at the  $k$ th step, which we do by prescribing that the probability of an orbit longer than  $k$  factorizes as

$$P_k(a_1 \dots a_n) = P(a_n | a_{n-k} \dots a_{n-1}) P_k(a_1 \dots a_{n-1}). \quad (19)$$

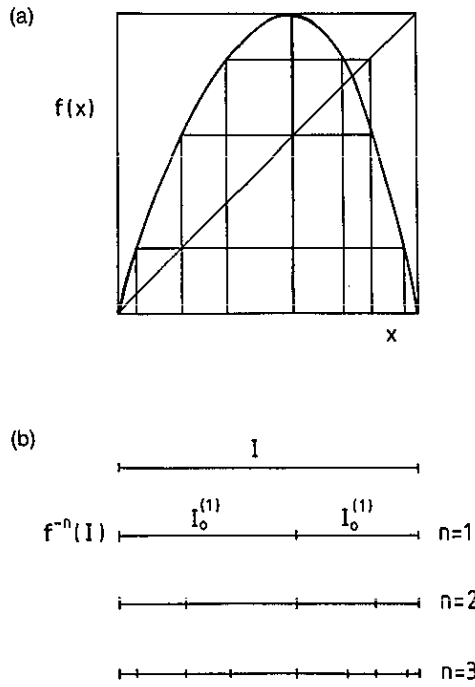


FIG. 1. Fully developed chaotic map with a smooth maximum. (a) Graph of the map. (b) A few generations of partitions,  $I_p^{(n)}$ ,  $n=1, 2, 3$ , as introduced in Sec. II C.

Note that the conditional probability  $P(a_n|a_{n-k}\cdots a_{n-1})$  depends only on the past up to the  $k$ th step, other arguments are neglected. For  $n \leq k$  the probability  $P_k(a_1 \cdots a_n)$  is equal to  $P(a_1 \cdots a_n)$ . The path probability  $P_k$  characterizes the truncated process. We can associate an entropy with the truncated symbolic process<sup>42-44</sup>

$$K_k^{tr} = \lim_{n \rightarrow \infty} K_{k,n} \tag{20}$$

$$K_{k,n} = -\frac{1}{n} \sum_{a_1 \cdots a_n} P_k(a_1 \cdots a_n) \ln P_k(a_1 \cdots a_n).$$

For  $n > k$  we have

$$K_{k,n} = (k+1)K_{k+1} - kK_k + \frac{k(k+1)}{n} (K_k - K_{k+1}), \tag{21}$$

where  $K_k$  is defined via (18), whence

$$K_k^{tr} = (k+1)K_{k+1} - kK_k. \tag{22}$$

Thus  $K_k^{tr} \rightarrow K$  and the difference between them measures the effect of neglecting memory in the symbolic dynamics. Below we demonstrate that the truncated entropies converge to the KS entropy in a typical chaotic 1D map exponentially, a result which has been rigorously proven for some types of maps.<sup>45</sup> We also show how the decay rate can be calculated. Equation (22) allows us to write  $K_n^{tr}$  in terms of subinterval measures

$$K_n^{tr} = \sum_p \mu(I_p^{(n+1)}) \ln \frac{\mu(f(I_p^{(n+1)}))}{\mu(I_p^{(n+1)})}. \tag{23}$$

At this point it is useful to convert to the equivalent Lebesgue map (16). That has the subintervals  $\tilde{I}_p^{(n+1)}$ , with their lengths  $\tilde{l}_p^{(n+1)}$  being their invariant measure. For  $n \rightarrow \infty$ ,  $K_n^{tr}$  converges to the KS entropy  $K$ , which now equals obviously the Lyapunov exponent, and expansion in terms of  $\tilde{l}_p^{(n+1)}$  yields the leading correction<sup>43</sup>

$$K_n^{tr} \approx K + \frac{1}{24} \sum_p \left( \frac{\tilde{f}''(x_p^{(n+1)})}{\tilde{f}'(x_p^{(n+1)})} \right)^2 (\tilde{l}_p^{(n+1)})^3, \tag{24}$$

where  $x_p^{(n+1)}$  is in the interval  $\tilde{I}_p^{(n+1)}$ . Due to mixing the terms under the sum decouple asymptotically, and one obtains

$$K_n^{tr} \approx K + bJ_n \tag{25}$$

with

$$J_n = \sum_p (\tilde{l}_p^{(n+1)})^3 \approx \int_I (\tilde{f}^{(n)'}(x))^{-2} dx. \tag{26}$$

Note that the above integral exists due to the fact that the equivalent Lebesgue map  $\tilde{f}$  does not have a critical point, i.e.,  $|\tilde{f}'(x)| > 0$ . We introduce a new quantity, the entropy decay rate defined by

$$\gamma = -\lim_{n \rightarrow \infty} \frac{1}{n} \ln J_n, \tag{27}$$

which tells us how rapidly  $K_n$  converges to  $K$ . As a forward reference, the decay rate  $\gamma$  is twice the Rényi entropy of order 3,  $\gamma = 2K(3)$ . The exponential convergence of  $K_n^{tr}$  means that the general asymptotic form of  $K_n$  is

$$K_n \approx K + \frac{1}{n} (A + Be^{-\gamma n} + \cdots), \tag{28}$$

where terms decaying with rates larger than  $\gamma$  were neglected. Whereas Eq. (28) might warrant a detailed discussion even at that stage, we restrict ourselves here to a few comments and as to details references are cited. The finite size corrections in (28) provide supplementary statistical characteristics on the system beyond that given by the KS entropy. The quantities  $\gamma$  and  $A$  can also be given the interpretation of different types of complexity.<sup>23,46,47</sup> On Fig. 3,  $K$  and  $\gamma$  are depicted for the case of the piecewise parabolic map (15). Note that in the weak intermittent limit,  $d=1$ , the entropy decay rate  $\gamma$  becomes zero, which is a sign of a dynamical phase transition (see Sec. IV C). We mention that the correlation decay rate [see Eq. (10)] is also zero at intermittency, in accordance with Refs. 36 and 37.

#### D. Perturbed maps

Double symmetric maps have invariants common with the tent map (12) and in some respect they can be considered as trivial ones. Although by the introduction of the transverse transformation on double symmetric maps (14) invariant probability densities of general FDC maps can be obtained, other properties such as correlation and entropy decay as well as generalized entropies and characteristics treated later in this paper are not easy to analyze. The

qualitatively new behavior of maps deviating from double symmetric ones is, however, expected to be highlighted by a perturbative approach.<sup>32,37,48,49</sup>

The basic idea of perturbation theory is similar to the one used in quantum mechanics, since in our case the question of determining a quantity is also often lead back to the spectral problem of an appropriately chosen operator. The main example treated in this section is the Frobenius–Perron operator, and subsequently various generalizations of it will be discussed. The operators corresponding to the tent map often have known spectra in a conveniently chosen function space. Then we perturb the map so as to move off double symmetry, construct the operator for the perturbed map, and finally calculate the perturbed spectrum and eigenfunctions order by order. Some technical details of the method can be found in Appendix A.

Concentrating on the Frobenius–Perron operator, its largest eigenvalue should stay constantly unity for any perturbation preserving the property of FDC, and the corresponding eigenfunction is just the natural invariant density for the perturbed map. The next-to-leading eigenvalue gives the correlation decay rate.

The perturbative method is illustrated here on the transverse maps (14), where we take  $v(x)$  for a small perturbation. Thus the map is

$$f(x) = f_L(x) - v(f_L(x)) + O(v^2), \quad (29)$$

and the invariant probability density is given in (14) exactly. First order perturbation theory gives for the correlation decay rate

$$r = -\ln |\lambda_1| = \ln 4 + \frac{1}{2}[v''(0) - 4v'(0)] + O(v^2). \quad (30)$$

For comparison we also give the Lyapunov exponent, the entropy decay rate together with its amplitude to lowest nontrivial order.<sup>43</sup> Using the notation

$$\Gamma = \int_I v'(x)^2 dx, \quad (31)$$

we have for the Lyapunov exponent and the entropy decay rate

$$L = \ln 2 - \Gamma/2 + \dots, \quad (32)$$

$$\gamma = \ln 4 - 3\Gamma + \dots, \quad (33)$$

where corrections are of  $O(v^3)$ . We also can show that for  $v(x) \equiv 0$   $B$  as defined by Eq. (28) vanishes, which is in accordance with the absence of relaxation in the tent map, where  $K_n^r = \ln 2$  for all  $n$ . It can be seen that the loss of double symmetry results in the decrease of the Lyapunov exponent  $L$ , while the correlation decay rate  $r$  may increase depending on the form of  $v(x)$ . Thus neither of the two indicators alone gives full information about the degree of stochasticity, demonstrating that the classification of deterministic disorder is a many-parameter problem, and one cannot speak about a single scale of randomness. Symbolic dynamics has lead to another characteristic rate  $\gamma$ , which is different from both the Lyapunov exponent and

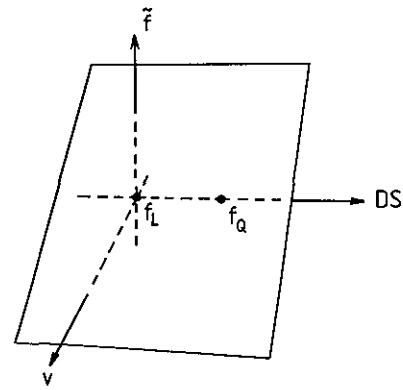


FIG. 2. Schematic plot of the space of FDC maps. The “surface” of symmetric maps is spanned by the double symmetric (DS) maps, and those transverse to the tent map ( $v$ ), see Eq. (14). All nonsymmetric maps can be obtained by conjugation from the symmetric “surface.” A sheet of equivalent maps, related by conjugation, is also depicted. Each such sheet contains one equivalent Lebesgue map  $f$ .

the correlation decay rate. In fact, symbolic dynamics give rise to a continuum of rates as we shall see in the thermodynamic treatment.

Another application of perturbation theory is demonstrated on the biquadratic map<sup>32,48</sup>

$$f_{BQ}(\epsilon, x) = 1 - (1 - \epsilon)(1 - 2x)^2 - \epsilon(1 - 2x)^4, \quad (34)$$

which shows FDC for  $-3/4 < \epsilon < 1$ . This map is conjugate to the transverse map (14), if we take  $v(x) = \epsilon(2\pi)^{-1} \sin \pi x$ . Thus the lowest-order results on invariants in terms of  $v(x)$  [see, e.g., Eqs. (32) and (33)] can be applied.<sup>34</sup> The invariant density is

$$P_{BQ}(\epsilon, x) = \pi^{-1}(x(1-x))^{-1/2} \left[ 1 + \epsilon(x-1/2) + \frac{3\epsilon^2}{4}(1-5x+4x^2) + \frac{\epsilon^3}{16}(160x^3-216x^2 + 60x+1) + O(\epsilon^4) \right]. \quad (35)$$

Knowing  $P_{BQ}(\epsilon, x)$ , the form of the transverse transformation and the conjugating function, which together connect the map (34) to the tent map, can be determined to the same order.

## E. The universal map of fully developed chaos

Whereas fully developed chaos can be perceived as a state remote from the onset of chaos in parameter controlled 1D maps, it emerges on different length scales at infinitely many parameter values, also near the onset. A notable sequence of such states consists of the band splitting points, where the attractor of  $2^{m-1}$  intervals split into  $2^m$  pieces.<sup>33,29</sup> This series can be considered as the mirror image of the period doubling sequence of attracting orbits reflected about the threshold point; here the period superimposed on the chaotic state doubles. The common accumulation point is approached by both sequences as char-

acterized by the Feigenbaum's universal ratio  $\delta_F = 4.669\dots$ .<sup>1</sup> By iteration and scaling the maps at the band splitting points can be brought to FDC form. For finite  $m$  those maps will depend on the specific form of the underlying parameter controlled map, in the limit  $m \rightarrow \infty$ , however, one obtains a universal FDC map  $f^*$ .<sup>31</sup> That map lies on the unstable manifold of Feigenbaum's fixed point function, and is the farthest from it among chaotic maps.

In the case of the logistic map  $rx(1-x)$  the first band splitting point  $m=1$  at  $r_1=3.678\dots$  corresponds to a biquadratic FDC map (34) with  $\epsilon=-0.295\dots$ . In the limit  $m \rightarrow \infty$  the universal FDC map is obtained as

$$f^*(x) = \sum_{i=0}^{\infty} \alpha_i x^{2^i}, \quad \sum_{i=1}^{\infty} \alpha_i = 0. \quad (36)$$

The coefficients  $\alpha_i$  are decreasing fast, thus the biquadratic form can be taken as a first approximation, which is supported by higher order calculations, too, and we have  $\epsilon^* = -0.262\dots$ .<sup>32</sup> Therefore, from the invariant characteristics calculated in this paper in lowest nontrivial order for the transverse map (14), we can read off the first approximation for the universal FDC map. We have the approximate universal value for the parameters  $\Gamma$  (31), the Lyapunov exponent (32), and the entropy decay rate (33)

$$\Gamma^* \approx 8.63 \times 10^{-3}, \quad L^* \approx 0.688, \quad \gamma^* \approx 1.338. \quad (37)$$

The last two numbers also play the role of the amplitudes in the asymptotic scaling forms for the invariants of parameter-controlled maps along the band merging sequence, i.e.,  $L_m \approx L^*/2^m$ ,  $\gamma_m \approx \gamma^*/2^m$ .

### III. TRANSIENT CHAOS

Signals exhibiting chaotic behavior on a finite time scale are called transiently chaotic. This phenomenon is associated with the existence of a fractal set in phase space which has, in contrast to chaotic attractors, a measure-zero basin of attraction. Such *nonattracting chaotic sets* repel trajectories from any finite neighborhoods of them, and the strength of this repulsion is inversely proportional to the average lifetime of chaos. (For a review see Ref. 24.)

One-dimensional maps are well suited for studying transient chaos not only since they provide the simplest examples but also because they model very closely what is going on along the unstable manifolds of strange chaotic sets in higher-dimensional systems with one-dimensional unstable manifold. In particular, the concept of the natural and of the so-called conditionally invariant measure, their properties and relation to each other can best be understood in 1D maps. In contrast to permanent chaos, nontrivial fractal features of the strange set show up already in one-dimensional transiently chaotic dynamics.

Transient chaos is generated by complete one-dimensional maps if a nonlinearity parameter exceeds the value belonging to the fully chaotic configuration (boundary crisis).<sup>30</sup> An interval  $I$  is mapped then under the dynamics  $x_{n+1}=f(x_n)$  partially *outside* itself, which implies, in general, a strong expansivity of the map. It is to be stressed that such maps can, in fact, be found in experi-

ments on transient chaos.<sup>50</sup> As an important class we shall consider here single humped functions, as illustrated in Fig. 4. It is irrelevant how the map looks for  $f(x)$  values outside  $I$ . In fact, there might be one or more attractors far away but if there is no feedback from these regions, the transient chaotic behavior is completely specified by the function  $f$  defined on  $I$ . The invariant set under  $f$  is a Cantor-set-like object and called *chaotic repeller*.<sup>51-55</sup>

The cylinder sets play an essential role in characterizing transient chaos, too.<sup>56</sup> Just as previously, they are defined at the  $n$ th level as the  $n$ th preimages of the support interval  $I$  and are denoted by  $I_i^{(n)}$ ,  $i=0,1,\dots,2^n-1$ . The novel feature is now that they do not cover the interval, rather for  $n \rightarrow \infty$  they approach a fractal set, the repeller.

#### A. Fractal dimension and the natural distribution on repellers

The fractal dimension is one of the most essential characteristics of chaotic repellers. It is remarkable that this number can be obtained as a particular parameter value in a generalized Frobenius-Perron equation. Let us consider first the original Frobenius-Perron equation (6) applied to a map  $f(x)$  generating transient chaos. Since the probability flows now out of the interval, any initial function will generate a decreasing series: The stationary density will be identically vanishing on  $I$ . In order to find convergence towards a finite limiting function the outflow is to be compensated. A local compensation can be done by raising  $f^i(x)$  to some power  $d$  less than 1. Considering the recursions

$$Q_n(x') = \sum_{x \in f^{-1}(x')} \frac{Q_{n-1}(x)}{|f'(x)|^d} \quad (38)$$

one finds that for very small values of  $d$  the iteration might even lead to an increasing series of  $Q_n(x)$ . Consequently, there must be an intermediate value of  $d$  at which the series of functions  $Q_n$  converges to a finite continuous function on  $I$  for any nonsingular  $Q_0$ . It has been shown<sup>26</sup> that this particular value coincides with the *fractal dimension*  $D_0$  of the repeller

$$d = D_0. \quad (39)$$

Equation (38) also provides a fast and accurate method for evaluating fractal dimensions of strange sets generated by one-dimensional maps. Numerically, one tries different values for  $d$  until a convergence sets in. Fortunately, the convergence, if present, is exponentially fast and the limit can be reached with good accuracy after a few steps.

Based on the analogy with the original Frobenius-Perron scheme, one expects that the limiting function  $Q(x)$  of Eq. (38) has an important meaning. In order to clarify this one has to define first the natural measure for chaotic repellers. Below we give a practical definition which can easily be used for constructing the natural measure in numerical simulations. In Sec. III B we show that the density of this measure on cylinder sets can be obtained from another extension of the Frobenius-Perron equation.

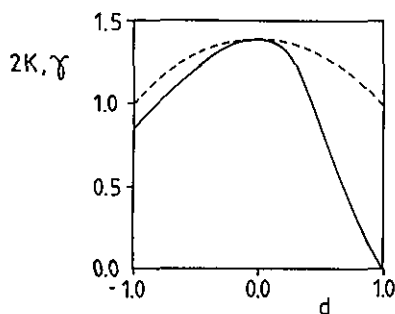


FIG. 3. The KS entropy and the entropy decay rate  $\gamma$  for the piecewise parabolic family given by Eq. (15).

Finally, we shall see that the function  $Q(x)$  is related to a coarse grained measure obtained by washing the natural measure out in boxes of equal size.

Since randomly chosen trajectories escape the interval  $I$  with probability one, the chaotic repeller or a tiny neighborhood of it can only be tested by using an *ensemble* of trajectories. The natural measure describes how often trajectories in the ensemble visit different pieces of the chaotic set. The algorithm given for constructing this measure is the following.<sup>52</sup> Distribute a large number of points on  $I$  (uniformly) and follow the trajectories starting out of them until they escape  $I$ . Only trajectories staying inside  $I$  sufficiently long are kept and even these are truncated: Some steps from the beginning and from the end are cut off in order to have their points lying really close to the repeller. A histogram made out of these points on a *uniform* grid of size  $\epsilon$  then provides a way of looking at the natural distribution which is subject to an error of order  $\epsilon$ .

As an illustrative example we use the logistic map at a parameter value which generates transient chaos. Figure 5 shows the approximate invariant measure on a repeller.

## B. Escape rate and the conditionally invariant measure

The *escape rate*<sup>51</sup> measures the strength of repulsion around the strange set. The number of survivors in an arbitrary neighborhood of the set decreases as time goes on and the decay is expected to be exponential for large  $n$ , i.e., to follow the rule  $\exp(-\kappa n)$ . The quantity  $\kappa$  is the escape rate, its reciprocal value can be considered to be the average lifetime of chaos. In one-dimensional maps, the total length of the cylinders at level  $n$  is just proportional to the number of trajectories staying inside  $I$  for at least  $n$  steps. Therefore, one has

$$\sum_{i=0}^{2^n-1} l_i^{(n)} \sim e^{(-\kappa n)}, \quad (40)$$

where  $l_i^{(n)}$  stands for the length of cylinder  $I_i^{(n)}$ .

We now introduce the *conditionally invariant* measure<sup>57</sup> which is strongly related to the natural one. The conditionally invariant measure (or *c-measure* for short) is defined on any region containing the repeller, and describes how trajectories escape this region. Consider the condi-

tional probability<sup>57</sup> that a given region is visited by trajectories (with random start in  $I$ ) which do not escape  $I$  in  $m$  steps. Note that certain trajectories exit already at the next step. Their last points are, therefore, far away from the repeller and fill in the gaps between cylinders. Consequently, the conditional probability is defined on the *entire* interval  $I$ . The limit to which this conditional probability converges for  $m \rightarrow \infty$  yields the conditionally invariant measure.

The c-measure can be considered as one maintained by pumping new points into the system exactly according to the rate they escape it [formally, by multiplying the number of points everywhere by a constant,  $\exp(\kappa)$ , in each step], so that an invariant distribution is obtained by means of a global compensation. The distribution tells us how often certain regions are visited in the system which is subject to the aforementioned flux of points.

It is easy to construct the conditional probability distribution for trajectories of minimal length  $m$  in the basic interval. One simply takes the algorithm used to construct the natural measure but does not discard the last steps of long living trajectories. Fortunately, the procedure converges exponentially fast. Figure 6 shows the result for our illustrative example.

To connect the conditionally invariant measure with the natural one let us *restrict*<sup>52,58</sup> the density of the c-measure to cylinders of level  $n$ . This, of course, requires a normalization such that the total measure on the cylinders is unity. The measures  $\mu_i^{(n)}$  of intervals  $I_i^{(n)}$  characterize then the motion of trajectories which end in one of the cylinders of level  $n$ . For  $n$  sufficiently large, these are the trajectories exhibiting long lived chaotic transients. Therefore, it is obvious that the limit of the conditionally invariant measure  $\mu_i^{(n)}$  obtained for  $n \rightarrow \infty$  can be considered as the *exact* natural measure on the repeller.<sup>52</sup>

For a deeper understanding it is essential that the density  $P(x)$  of the conditionally invariant measure can be obtained also by *analytic* means. As shown in Refs. 57 and 59 the density follows from the iteration scheme

$$P_n(x') = R \sum_{x \in f^{-1}(x')} \frac{P_{n-1}(x)}{|f'(x)|}. \quad (41)$$

By iterating any nonsingular positive initial function  $P_0(x)$  on  $I$ , the series  $P_n(x)$  will diverge or die out unless the coefficient  $R$  takes the value

$$R = e^\kappa. \quad (42)$$

With this  $R$  the series  $P_n(x)$  converges towards a finite continuous  $P(x)$  which is *independent* of the choice of the initial function, provided it is nonsingular. One, thus, simultaneously finds both escape rate and density  $P(x)$  from an eigenvalue problem.

Technically, the density  $P(x)$  of the c-measure is the analog of the invariant density of FDC maps, and averages, correlation functions, etc., can be computed by means of  $P(x)$ , after restricting it to the cylinders.<sup>58</sup>

By iterating (41) one clearly sees that a singularity builds up at the maximum of  $f(x)$  but it is *outside* of  $I$ . This shows that the density of the conditionally invariant

measure is, in general, a nonsingular function on close neighborhoods of chaotic repellers. Consequently, the dynamical system can typically be considered to be *hyperbolic*. (We call a map hyperbolic if there is an iterate of  $f$  for which the modulus of the slope is everywhere larger than unity.) This hyperbolicity of chaotic repellers will be assumed in what follows if not stated otherwise. Since the density does not change with the refinement, the asymptotic scaling in  $n$  will be governed by the length scales alone. Thus one finds the simple statement that *the measure  $\mu_i^{(n)}$  of a cylinder is proportional to its length*, more precisely

$$\mu_i^{(n)} \sim l_i^{(n)} / \sum_j l_j^{(n)} \sim e^{\kappa n} l_i^{(n)}. \quad (43)$$

This relation will play an essential role in what follows. In particular, measure  $\mu_i^{(n)}$  is the probability to find trajectories of length  $n$  having a given type of symbolic codes. When computing the entropies for transiently chaotic trajectories one can thus use the  $\mu_i^{(n)}$ 's as the path probabilities. These properties of the natural and c-measures have widely been used in studying transient chaos in higher-dimensional systems.<sup>60,61</sup>

Let us finally return to the relation between the limiting function  $Q(x)$  of (38) and the natural measure. As we saw, the exact determination of the natural measure goes via an ever refining cylinder set. In practice one is often interested in a coarse grained measure obtained by vashing the natural measure out on a grid of size  $\epsilon \ll 1$ , with  $\epsilon$  fixed. It turns out<sup>26</sup> that this coarse grained measure possesses a nonsingular covering curve (see Fig. 5) which is then proportional not to the density  $P(x)$  of the conditionally invariant measure but rather to the function  $Q(x)$  obtained from (38) as  $n$  goes to infinity.

Exceptionally, chaotic repellers might be nonhyperbolic when, e.g., one branch of  $f(x)$  happens to have a smooth maximum, which is mapped in two steps into the origin.<sup>62</sup> The density  $P(x)$  of the c-measure is then singular in the endpoints very much in the same manner as the natural measure in nonhyperbolic FDC maps. Such cases will be discussed in Sec. IV A and IV C.

### C. Multifractal properties

Equations (38) and (41) can be considered as two different solution to the problem of how the outflow of probability described by the Frobenius–Perron equation can be compensated around a chaotic repeller. In Eq. (38) the exponent of  $f'(x)$  was chosen to be different from unity, while in Eq. (41) a global prefactor was introduced by keeping the original exponent. One might also try to apply these two types of compensation simultaneously. This means that for any exponent different from  $D_0$  there exists a unique prefactor so that the new iteration scheme converges towards a finite limiting function. For repellers one can always choose the prefactor in the form of  $\exp(\kappa q)$  with an arbitrary real  $q$ . The corresponding exponents were

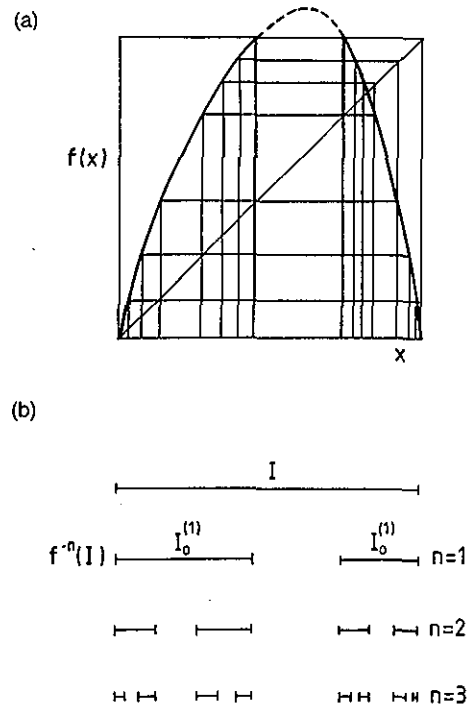


FIG. 4. Typical map generating transient chaos on some interval  $I$ . Note that points lying outside the two subintervals  $I_0^{(1)}$  and  $I_1^{(1)}$  escape  $I$  after one time unit. Points which do not exit in  $n$  steps are contained in the  $n$ th preimages of  $I$ , and exhibit chaotic behavior, on time scale  $n$ . Cylinder sets up to level 3 are shown in the lower part of the figure.

found<sup>63–65</sup> to be related with the order- $q$  generalized dimensions  $D(q)$  (Refs. 4 and 5) taken with respect to the natural measure. More precisely,

$$Q_{n+1}(x') = e^{\kappa q} \sum_{x \in f^{-1}(x')} \frac{Q_n(x)}{|f'(x)|^{q-(q-1)D(q)}} \quad (44)$$

is a compensated recursion leading to a finite limiting  $Q$ . This recursion can be used to determine  $D(q)$  with high accuracy.

From the point of view of dynamical systems, natural measures are the most essential ones. There exist, however, entire classes of invariant measures different from the natural one which can play an important role when considering maps appearing in other physical context.

An interesting family of invariant measures on repellers, and on attractors of FDC maps, obtained by iterating the map *backward* in a *random* manner. Different distributions arise because of different ways of backward iteration. To each value  $x$  belong two preimages (if the map is single humped) denoted by  $f_r^{-1}(x)$  where  $r=1$  if the preimage belongs to subinterval  $I_0^{(1)}$ , and  $r=2$  otherwise. The probability for taking branch 1 or 2 is to be decided. We suppose this depends on the actual position only and denote by  $p_1(x)$  the probability for choosing branch 1. Obviously,  $p_2(x) = 1 - p_1(x)$ . The resulting distribution is a multifractal, the dimensions of which were shown<sup>65</sup> to be obtainable from the recursion scheme

$$Q_{n+1}(x) = \sum_{r=1}^2 \frac{Q_n(f_r^{-1}(x))p_r^q(x)}{|f_r'(f_r^{-1}(x))|^{(1-q)D(q)}}. \quad (45)$$

The associated nonnatural measures might be the physically relevant ones in applications beyond the scope of dynamical systems (see Appendix B).

#### D. The period doubling attractor as a repeller

As an example, we show here how the fractal properties of the Feigenbaum (or period doubling) attractor can be studied by means of the methods worked out for complete maps. It is a relatively recent observation<sup>66</sup> that the Feigenbaum attractor as a geometrical object appears also as a *repeller* of a map  $f_u$  which can be expressed via universal quantities. The function  $f_u$  for the quadratic map family consists of a straight line branch  $f_u(x) = \alpha_F x$  with  $\alpha_F = -2.5029\dots$  being a universal scaling exponent and a somewhat curved branch  $f_u(x) = \alpha_F g(x)$ . The function  $f_u$  is defined on the interval  $I = (1/\alpha_F, 1)$  (Fig. 7).

Cylinders generated by the preimages of  $I$  provide also a coverage of the attractor. One must, however, be careful when trying to study *metric* properties, since the natural measure of the repeller is not the same as that of the attractor! The natural measure on the attractor is generated by the forward iterates of the maximum point under map  $g$ . It is easy to check that this trajectory visits equally often all cylinders of level  $n$ , consequently, the natural measure on the attractor must be the same in all cylinders. This can also be obtained by iterating map  $f_u$  backward with equal probabilities.

The most important quantity is the set of dimensions. One can determine  $D(q)$  from the eigenvalue equation (45) with  $p_1 = p_2 = 1/2$ . By using high order polynomial expansions for  $g(x)$ , the generalized dimension of the period doubling universal attractor could be determined by this method with ten digits accuracy.<sup>67</sup> A method yielding even better accuracies is based on a zeta function constructed from the primitive cycles of the map  $f_u$ .<sup>68</sup>

#### IV. THERMODYNAMIC FORMALISM

Based on classical mathematical papers,<sup>11-13</sup> the thermodynamic formalism for chaotic systems has recently become a common tool both for mathematicians<sup>69-74</sup> and for physicists.<sup>75-87</sup> Here we show how the basic concepts work in one-dimensional maps exhibiting fully developed and transient chaos. For this class an explicit form of Ruelle's Frobenius-Perron operator can be found providing a powerful method for computing characteristics, like the free energy, the Rényi entropies, and their decay rates. Because nonhyperbolic cases are also treated, different kinds of eigenvalue problems and operators are found, generalizing thus the "classical" results. As a consequence of nonhyperbolicity, nonanalytic behaviors, phase transitions, show up in the characteristics. The ones found in the entropies seem to be of a very general nature which can also be found in higher-dimensional cases and in systems not directly related with chaotic phenomena, too.

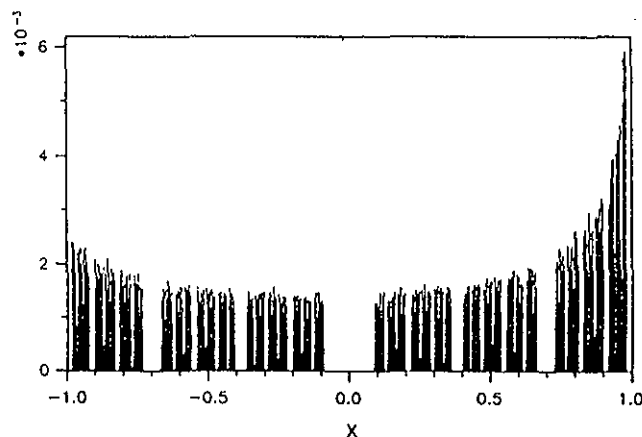


FIG. 5. Natural distribution for map  $x_{n+1} = 1 - 2.05x_n^2$  obtained on a grid of size 0.002. The number of initial points distributed uniformly on  $I$  was  $10^7$ , and the first 10 and the last 30 steps of trajectories were discarded. The truncated trajectories contained about  $10^6$  points ensuring a very good statistics.

#### A. Thermodynamical quantities

In analogy with different multifractal spectra, one might wish to make a direct characterization of the measure distribution of the cylinders by raising the measures to a certain real power  $\beta$  and summing them all up at level  $n$ . An exponential scaling is expected for the partition sum<sup>21</sup>

$$Z_{\mu,n}(\beta) \equiv \sum_i \mu_i^{(n)\beta} \sim e^{-\beta F_\mu(\beta)n}, \quad (46)$$

for  $n \rightarrow \infty$ , where  $F_\mu(\beta)$  is a kind of free energy. This notation is motivated by an analogy between the binary code associated with a given cylinder at level  $n$  and the microstate of an Ising chain of length  $n$ .  $\beta$  plays the role of the inverse temperatures  $\mu^{(n)\beta}$  is the Boltzmann factor and  $F_\mu$  corresponds to the free energy per spin of the Ising chain with typically long-range and multispin interactions. In what follows it will be understood that  $\mu$  is the natural measure.

A similar quantity can be defined through another partition sum<sup>56</sup>

$$Z_n(\beta) \equiv \sum_i I_i^{(n)\beta} \sim e^{-\beta F(\beta)n}, \quad (47)$$

where  $F(\beta)$  is a different free energy, which characterizes the length scale distribution of the cylinders. [In the case of hyperbolic systems  $-\beta F(\beta)$  agrees with the topological pressure introduced in the mathematical literature.<sup>11-13</sup>]

For hyperbolic maps the measure is proportional to the length [see Eq. (43)] and the two free energies are then related as

$$F_\mu = F - \kappa. \quad (48)$$

In permanently chaotic cases ( $\kappa=0$ ) they coincide if the map is hyperbolic otherwise the difference between the free energies is a measure of nonhyperbolicity.

It is a recent development that these free energies can be obtained from the largest eigenvalues of a generalized

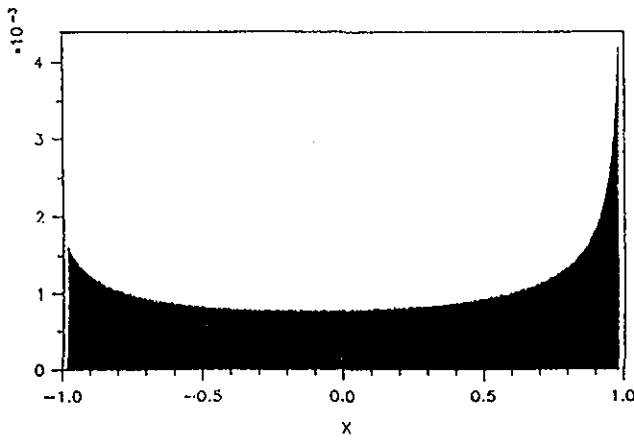


FIG. 6. The conditionally invariant measure for map  $x_{n+1}=1-2.05x_n^2$  obtained by discarding the first 10 steps of trajectories and plotting the distribution of all points which stay inside the basic interval. Parameter, initial conditions, and box size are the same as in Fig. 5.

Frobenius–Perron (GFP) operator  $H(\beta)$  (Refs. 26–28, 22, 66, and 82–87), which is the transfer matrix of the infinite Ising chain mentioned above. The operator  $\hat{H}_h(\beta)$  of map  $h(x)$  acts on any function  $Q(x)$  defined on  $I$  as follows

$$\hat{H}_h(\beta)Q(x') = \sum_{x \in h^{-1}(x')} \frac{Q(x)}{|h'(x)|^\beta} \quad (49)$$

The spectrum of this operator depends on the function space from which  $Q(x)$  is chosen. Here and in the following we shall concentrate on functions which are generated by subsequent applications of  $\hat{H}_h$  to a nonsingular positive  $Q_0$  on  $I$ . The largest eigenvalue  $\lambda_0^{(h)}(\beta)$  belonging to this class can be obtained from the relation

$$\hat{H}_h^n(\beta)Q_0(x) \approx \lambda_0^{(h)n}(\beta)Q(x) \quad (50)$$

for  $n \rightarrow \infty$ , where  $Q(x)$  is the corresponding eigenfunction.

Based on the observation that the slope of the  $n$ -fold iterated map  $f^n(x)$  in cylinder  $i$  is inversely proportional to the length  $l_i^{(n)}$ , one can show<sup>27,66,82</sup> that the free energy  $F(\beta)$  is connected with the largest eigenvalue of the GFP operator of map  $f(x)$  as

$$\lambda_0^{(f)}(\beta) = e^{-\beta F(\beta)}. \quad (51)$$

It is worth emphasizing that this result holds for both hyperbolic and nonhyperbolic and for both permanently and transiently chaotic maps.

Equations used in Sec. III are special cases of Eqs. (49) and (51). Iteration schemes (38) and (41) can be viewed now as expressions of the general relations

$$F(D_0) = 0 \quad \text{and} \quad F(1) = \kappa, \quad (52)$$

respectively.

Analogously, one obtains the free energy  $F_\mu(\beta)$  of an FDC map  $f(x)$  from the largest eigenvalue of the GFP operator which we take now with the equivalent Lebesgue map  $\tilde{f}(x)$  defined by Eq. (16):<sup>22</sup>

$$\lambda_0^{(\tilde{f})}(\beta) = e^{-\beta F_\mu(\beta)}. \quad (53)$$

This follows from the fact that the cylinder lengths of  $\tilde{f}$  are just the natural measures of the corresponding cylinders of the original map  $f$ , and the measures are invariant under conjugations.

It is instructive to see another operator,<sup>22</sup> expressed completely in terms of the original map  $f(x)$ , which also yields  $\lambda_0^{(f)}(\beta)$  as its largest eigenvalue in the class of functions defined above. This operator  $\hat{H}_f(\beta, \beta)$  acts as

$$\hat{H}_f(\beta, \beta)Q(x) = P^{-\beta}(x)\hat{H}_f(\beta)[P^\beta(x)Q(x)], \quad (54)$$

where  $P(x)$  is the density of the invariant measure. It is worth noting that the extra weighting factors  $P^\beta(x)$  ensure the correct scaling of the natural measure in the outermost cylinders, where in nonhyperbolic cases a singularity shows up, and the measure is thus not proportional to the length. This result is expected to also hold in the case of both hyperbolic and nonhyperbolic repellers when  $P(x)$  stands for the density of the  $c$ -measure.

The free energy  $F_\mu(q)$  is related to the Rényi entropy  $K(q)$  (Refs. 7 and 8) that have been introduced as dynamical invariants which give a more detailed description of the dynamics than the single KS entropy alone. Applying the general definitions<sup>8</sup> which contains a sum of the  $q$ th power of the path probabilities, one finds  $K(q)$  to be closely related to the growth rate of the partition sum  $Z_{\mu,n}(q)$ . In particular,

$$K(q) = \frac{qF_\mu(q)}{q-1}. \quad (55)$$

In other words, apart from a trivial factor, the order  $q$  Rényi entropy is equal to the free energy  $F_\mu(q)$ . Provided  $K(q)$  is analytic around  $q=1$ , the order 1 Rényi entropy is found to be the KS entropy defined in (18). We shall see, however, that analyticity might break down, therefore, it is better to accept  $K(1)$  to be by definition the KS entropy.

A more detailed description of the hierarchic structure of chaos can be given if instead of (46) or (47) a partition sum  $\sum \mu_i^{(n)q} l_i^{(n)\beta}$  is considered containing both the lengths and the measures of cylinders. Since essential difference in the scaling behavior of these quantities can be found in the outmost cylinders only, the partition sum goes, in leading order, as the  $n$ th power of the largest eigenvalue of an operator  $\hat{H}_f(q+\beta, q)$ , where the operator  $\hat{H}_f(r, s)$  is defined by

$$\hat{H}_f(r, s)Q(x) = P^{-s}(x)\hat{H}_f(r)[P^s(x)Q(x)]. \quad (56)$$

Here  $\hat{H}_f(q)$  is the GFP operator (49) taken with map  $f$ , and  $P(x)$  stands either for the invariant density or for the density of the  $c$ -measure. Instead of working out the corresponding bivariate thermodynamics<sup>62,79,88–90</sup> in detail, we shall concentrate on two important special cases.

First, let us introduce the spectrum  $L(q)$  of local Lyapunov exponents.<sup>9,10</sup> Since  $1/l_i^{(n)}$  is the local expansion factor in cylinder  $I_i^{(n)}$ , a weighted average of their  $q$ th power taken with respect to the natural measure defines an order  $q$  expansion rate  $L(q)$  via

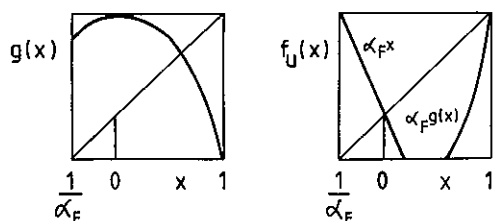


FIG. 7. A schematic plot of the universal map  $f_u$ . The invariant set of  $f_u$  is the period-doubling attractor. In reality, the branch  $\alpha_F g(x)$  is much closer to a straight line. For comparison, the Feigenbaum fixed point function  $g(x)$  is also shown.

$$\sum_i l_i^{(n)-q} \mu_i^{(n)} \sim e^{qL(q)n}. \quad (57)$$

The case  $q \rightarrow 0$  corresponds to the average Lyapunov exponent  $L(0) = K_1 + \kappa$ . Next consider  $\hat{H}_f(1-q, 1)$  which is a generalization for nonhyperbolic maps of the operator introduced by Fujisaka and Inoue.<sup>28</sup> Because of (57), the largest eigenvalue of this operator is  $\exp(qL(q) - \kappa)$ .

The generalized dimensions  $D(q)$  (Ref. 4) taken with respect to the natural measure fulfill the relation<sup>5</sup>

$$\sum_i l_i^{(n)-\tau(q)} \mu_i^{(n)q} \sim 1 \quad (58)$$

when  $\tau(q) = (q-1)D(q)$ . Consequently, the order  $q$  generalized dimension can also be obtained from the special choice  $\tau^*(q)$  for which the largest eigenvalue of  $\hat{H}_f(q - \tau^*(q), q)$  is just  $\exp(-\kappa q)$ . Since the sums (57) and (58) contain length scales, the quantities  $L(q)$  and  $D(q)$ , just like the free energy  $F(\beta)$  [Eq. (47)], are not invariant under singular coordinate transformations. Note, however, that by replacing the length scales  $l_i^{(n)}$  with any (nonnatural) invariant measure  $\nu_i^{(n)}$  of map  $f(x)$  one could introduce a bivariate partition sum taken over cylinders with nonzero measures  $\sum_i \mu_i^{(n)q} \nu_i^{(n)\beta}$ , and quantities derived from equations similar to (57) and (58) would then be invariant under any conjugation.

When comparing operators  $\hat{H}(\beta)$  and  $\hat{H}(r, s)$ , one can clearly see that the quantities  $F(\beta)$ ,  $K(\beta)$ ,  $L(1-\beta)$ , and  $D(q=\beta)$  can be independent in nonhyperbolic cases. The difference between these spectra can also be viewed as the difference in the action of the GFP operator  $\hat{H}_f$  on function spaces with different singularities at the outmost points of  $I$ . [The latter are induced by the weighing factors  $P^\beta$  and  $P^s$  in Eqs. (54) and (56), respectively.] In hyperbolic cases, however,  $P(x)$  is a nonsingular positive function on  $I$ , the spectra of the operators mentioned above coincide, and from the largest eigenvalue one finds

$$\beta F(\beta) = \kappa\beta + (\beta-1)K(\beta) = \kappa - (1-\beta)L(1-\beta), \quad (59)$$

and

$$\beta F(\beta)|_{\beta=q-(q-1)D_q} = \kappa q. \quad (60)$$

The last relationship is expressed in the language of recursions as Eq. (44). We note, however, that even in nonhyperbolic cases these relations hold in certain regions of the inverse temperature.

A perturbation theory can be worked out for all the Frobenius–Perron type operators introduced above in a similar manner as presented in Sec. II D and in Appendix A. In particular, the entropies have been computed near a map with known properties.<sup>20,22</sup> For the maps (14) the first correction reads

$$K(q) = \ln 2 - q(\Gamma/2) + \dots, \quad (61)$$

where  $\Gamma$  is given by (31). A high-order calculation is illustrated in Fig. 8 together with the result of the numerical simulation.

An equivalent description is given by the dynamical multifractal spectrum  $g(\Lambda)$  which is connected to  $(q-1)K(q)$  by means of a Legendre transformation<sup>6,91,92</sup>

$$(q-1)K(q) = \min_{\Lambda} (q\Lambda - g(\Lambda)). \quad (62)$$

In leading order for the maps (14) one obtains<sup>20</sup>

$$g(\Lambda) \approx \ln 2 - \frac{(\ln 2 + \Gamma/2 - \Lambda)^2}{2\Gamma}. \quad (63)$$

This shows that  $\Gamma$  is just the halfwidth of the spectrum near its maximum. By using the value (37) for  $\Gamma^*$ , one obtains the dynamical multifractal spectrum valid for the universal FDC map.

## B. Approach to the thermodynamic limit

The manner in which quantities obtained from cylinder properties at level  $n$  tend to the asymptotic expressions  $F(\beta)$ ,  $K(q)$ , or  $L(q)$  valid in the thermodynamic limit  $n \rightarrow \infty$  is an internal characteristic of the chaotic system. This also has a practical relevance since the velocity of the approach determines essentially the accuracy with which the asymptotic quantities can be obtained from a finite  $n$  calculation. Because of the prefactors not written out on the right-hand side of the scaling relations like, e.g., (46), a general  $1/n$  dependence is present in the asymptotical quantities. The next correction is expected to be exponential provided the largest eigenvalue of the operator in question is separated by a gap from the rest of the spectrum. If these assumptions are not fulfilled, a critical slowing down occurs in the approach to the thermodynamical quantities which signals the existence of nonanalyticities, phase transitions, what we shall discuss in Sec. IV C. Here we work out in some detail the decay process associated with the Rényi entropies, the characteristics being invariant under the most general form of transformations.

Let us define the finite time Rényi entropies  $K_n(q)$  via relation

$$K_n(q) = \frac{1}{1-q} \frac{1}{n} \ln Z_{\mu,n}(q), \quad (64)$$

where the partition sum is defined by Eq. (46). One is interested in how  $K_n(q)$  is approaching  $K(q)$  for  $n \rightarrow \infty$ .

Next, introduce the asymptotic quantities<sup>7,23</sup>

$$I_{q,K} = \lim_{n \rightarrow \infty} n(K_n(q) - K(q)), \quad (65)$$

which are called reduced dynamical Rényi informations of order  $q$ . It is obvious from the definition that the reduced dynamical Rényi informations are just the amplitudes of the  $1/n$  corrections.

A typical next-to-leading-order asymptotics of  $K_n(q)$  is<sup>23</sup>

$$K_n(q) \sim K(q) + \frac{I_{q,K} + B(q)\delta^n(q)}{n}, \quad n \rightarrow \infty, \quad (66)$$

where  $|\delta(q)|$  is less than unity. Situations where in some region of  $q$  this asymptotics is not valid is discussed in Sec. IV C. The quantity,

$$\gamma(q) = -\ln|\delta(q)|, \quad (67)$$

is called generalized entropy decay rate and  $1/\gamma(q)$  can be considered to be the relaxation time of  $K_n(q)$ .<sup>22</sup> The entropy decay rate  $\gamma$  defined in Sec. II C corresponds to  $q=1$ .

For piecewise analytic FDC maps it has been found<sup>22</sup> that  $K_n(q)$  has two competing relaxation terms for  $q \neq 0, 1$ . Both are closely related to the eigenvalues of the generalized Frobenius–Perron operator  $\tilde{H}_{\tilde{f}}$ . One decay process is governed by the second largest eigenvalue  $\lambda_1^{(f)}(q)$ , as expected. Another, nontrivial decay process is due to finite size effects, to the fact that the cylinder lengths are expressible only in leading order as the derivative of the  $n$ -fold iterated map. This rate turns out to be connected with the largest eigenvalue but taken at an inverse temperature shifted by 2. Both processes are of equal importance, therefore,  $\delta(q)$  proves to be a maximum of two terms

$$|\delta(q)| = \max \left( \left| \frac{\lambda_1^{(f)}(q)}{\lambda_0^{(f)}(q)} \right|, \left| \frac{\lambda_0^{(f)}(q+2)}{\lambda_0^{(f)}(q)} \right| \right). \quad (68)$$

Since the largest eigenvalue is related to the entropies, the order  $q$  decay rate is either the negative logarithm of the ratio of the two leading eigenvalues or can be given in terms of the entropies themselves as  $(q+1)K(q+2) + (1-q)K(q)$ . At  $q=1$  the contribution of  $\gamma$  comes always from the latter term since in the expansion of  $Z_{\mu,n}(q)$  in terms of the eigenvalues the amplitude of  $\lambda_1^n(q)$  vanishes. For  $q=0$  none of the relaxation processes are present due to the complete grammar of the symbolic dynamics.

The perturbation expansion can be extended to  $\gamma(q)$  as well. Here we quote, as in Sec. II D, results obtained<sup>22,35</sup> in leading order in the perturbing function  $v(x)$  [Eq. (14)]

$$\gamma(q) = \min(\ln 4 + qv''(0)/2 - (q+1)v'(0), \ln 4 - (2q+1)\Gamma) \quad (69)$$

valid for  $q \neq 1$ , where  $\Gamma$  is defined by Eq. (31). The contribution coming from the second largest eigenvalue is the first expression inside the parenthesis. Since it is never present at  $q=1$ , the result  $\gamma(1) = 2K(3)$  might appear as an isolated point in the graph of  $\gamma(q)$  depending on the

actual form of  $v(x)$ . For the universal FDC map the entropic contribution dominates for  $|q-1| \ll 1$  and the universal entropy decay rates then read as

$$\gamma^*(q) \approx \ln 4 - (2q+1)\Gamma^*, \quad (70)$$

where  $\Gamma^*$  has been defined in Eq. (37).

### C. Phase transitions

Phase-transition-like phenomena are much more seldom in  $K(q)$  than in other characteristics, due to the strong invariance property of the entropies against conjugation. They occur at border line situations of chaos. In other thermodynamical formalisms [as, e.g., the ones based on the free energy  $\beta F(\beta)$ , or the Lyapunov exponents  $L(q)$ ] phase transitions away from borderline situations show up in nonhyperbolic maps. In such cases the two leading eigenvalues of the relevant GFP operator coincide at the critical point and the corresponding decay rate vanish. These phase transitions, however, are not invariant under singular coordinate changes that cancel or create a critical point. Furthermore, phase transitions, due to similar effects, have been observed in the generalized dimensions of higher-dimensional systems. For these problems see the reviews<sup>14–19</sup> and references therein.

In what follows we concentrate on the most robust phase transitions, i.e., the ones in the entropies, which simultaneously always occur in all other thermodynamic quantities. Such cases have in common that the leading behavior of partition sums like (46) is *not exponential* in certain regions of  $\beta$ . Furthermore, we shall point out that these transitions are also reflected in the singular behavior of  $I_{q,K}$  and  $\gamma(q)$ . The borderline situations which are the reason for these phase transitions correspond to marginal stability (intermittency) or super instability of the dynamics. In 1D maps conjugated to the tent map no phase transition can show up. By applying an operation transverse to conjugation, these borderline situations are found if  $v'(0)=1$  and if  $v'(0)=-1$  in Eq. (14) when the fixpoint in the origin becomes marginally unstable [i.e.,  $f'(0)=1$ ] and superunstable [i.e.,  $f'(0)=\infty$ ], respectively. In both cases a well defined density exists according to Eq. (14). In what follows we restrict our attention to permanently chaotic maps.

#### 1. Intermittency

The first possibility  $f'(0)=1$  means that the dynamical system is in a weak intermittent state.<sup>36</sup> An example is the map (15) at  $d=1$ . Close to the intermittent state, the form of the map near the origin is

$$f(x) = (1+\eta)x + ax^2 + \dots, \quad \tilde{z} > 1. \quad (71)$$

It is worth also giving how the equivalent Lebesgue map  $\tilde{f}(x)$  [Eq. (16)] behaves:

$$\tilde{f}(x) = (1+\tilde{\eta})x + \tilde{a}x^2 + \dots, \quad \tilde{z} > 1. \quad (72)$$

Here  $\eta, \tilde{\eta} \geq 0$  and equality holds at weak intermittency.

The existence of a phase transition follows from an upper bound for the Rényi entropies<sup>20,21,23</sup>

$$K_n(q) < \frac{q}{q-1} \lim_{n \rightarrow \infty} \frac{1}{n} \ln \frac{1}{\mu(I_0^{(n)})}, \quad q > 1. \quad (73)$$

This is obtained by keeping the contribution of the leftmost interval only in the partition sum (46). One can show, however, that this measure now decays as a power law<sup>43</sup>

$$\mu(I_0^{(n)}) \sim n^{-1/(\tilde{z}-1)}, \quad (74)$$

where  $\tilde{z}$  is fixed by Eq. (72). Consequently,  $K(q) \equiv 0$  for  $q > 1$ . Recall that our system is chaotic, i.e.,  $K \equiv K(1)$  is strictly positive by definition. Since  $K(q)$  is monotonously decreasing with increasing  $q$ , we have two regions<sup>20,21,23</sup> as shown in Fig. 9(a):

$$\begin{aligned} K(q) > 0, \quad q < 1, \quad \text{“normal chaos phase,”} \\ K(q) = 0, \quad q > 1, \quad \text{“regular chaos phase,”} \end{aligned} \quad (75)$$

The regular chaos region  $q > 1$  is dominated by the “condensed,” seemingly regular behavior of trajectories coming close to the origin. At the critical temperature  $q_c = 1$  we have a jump in the entropy spectrum, which is equal to the Kolmogorov–Sinai entropy. An analysis of an extended statistical physics of this phase transition has been worked out in<sup>93–97</sup> subsequently.

An analogous phenomenon can be seen in systems exhibiting self-organized critical behavior. Such systems are in a marginally unstable state and their temporal correlations decay according to a power law. Correspondingly, in a cellular automaton model showing this behavior, the existence of the same phase transition was pointed out.<sup>98</sup>

In accordance with (75) and (62),  $g(\Lambda) = \Lambda$  in the range  $0 < \Lambda < K(1)$ , and this part of the  $g(\Lambda)$  curve then joins a single humped curve with a continuous first derivative [see Fig. 9(c)].

According to the definition (65), one obtains<sup>23</sup> for the reduced dynamical Rényi information the lower bound

$$I_{q,K} \geq I_{\infty,K} = \lim_{n \rightarrow \infty} \ln \frac{1}{\mu(I_0^{(n)})}, \quad q > 1. \quad (76)$$

Consequently,  $I_{q,K} = \infty$  in the regular phase. In the normal phases  $I_{q,K}$  is finite and diverges to  $-\infty$  as  $q \rightarrow 1-0$ .

It is worth noting that the limit  $\eta \rightarrow 0$  (implying  $\tilde{\eta} \rightarrow 0$ ) resembles a phase transition,  $\eta$  playing the role of a control parameter. Approaching the critical point along the path  $q = q_c = 1$ ,  $\eta \rightarrow 0$ , the entropy decay rate (27) reflects a critical slowing down. The characteristic relaxation time then diverges<sup>43</sup> as

$$\tau = \frac{1}{\gamma} = \frac{1}{\tilde{\eta}(2\tilde{z}-1)}. \quad (77)$$

At the point  $\eta = 0$  the entropy  $K_n(1)$  decays algebraically.<sup>43,37,45</sup>

To follow the behavior along the “temperature” direction at  $\eta = 0$ , the entropy decay  $\gamma(q)$  is positive for  $q < q_c$  and  $\gamma(q)$  tends to zero<sup>22</sup> when  $q \rightarrow 1-0$ , exhibiting the critical slowing down again. In the regular phase  $\gamma(q) = 0$ .

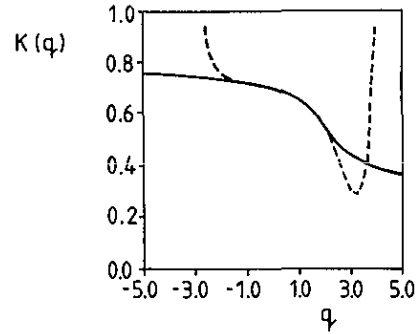


FIG. 8. Rényi entropies of the map (15) at  $d=0.5$ . Solid and dashed lines show the results of a numerical calculation and of the perturbation expansions, respectively, carried out up to 9th order in  $d$ .

## 2. Super instability

Next, let us investigate the opposite case, when the map (14) has a super unstable fixpoint [ $f'(0) = \infty$ ] at the origin. An example for such a map is (15) at  $d = -1$ . In that case the probability that the trajectory stays up to time  $n$  in the neighborhood of the origin decreases faster than exponentially<sup>23</sup> as a function of  $n$ . In particular,

$$\mu(I_0^{(n)}) \sim B^{-C^n} \quad (78)$$

with constants  $B > 1$  and  $C > 1$ .

A lower bound for  $K(q)$  in the region  $q < 0$  can be obtained<sup>35,23</sup> by keeping only the probability (78) in the partition sum (46) as

$$K(q) \geq \frac{q}{q-1} \lim_{n \rightarrow \infty} \ln \frac{1}{\mu(I_0^{(n)})} = \infty, \quad q < 0. \quad (79)$$

Since the topological entropy  $K(0) = \ln 2$  and  $K(q) < K(0)$  for  $q > 0$ , one has a singularity in  $K(q)$  again. This is, however, completely different from the previous one. The two phases shown in Fig. 9(b) are now characterized by<sup>35,23</sup>

$$\begin{aligned} K(q) = \infty, \quad q < 0, \quad \text{“anomalous phase,”} \\ K(q) < \infty, \quad q \geq 0, \quad \text{“normal chaos phase.”} \end{aligned} \quad (80)$$

An infinite jump can be seen in  $K(q)$  at  $q_c = 0$ . The dynamical multifractal spectrum  $g(\Lambda)$ , defined in (62), in this situation has the particular property that reaches its maximum value [the topological entropy  $K(0)$ ] at  $\Lambda = \infty$ , and the decreasing branch of the curve is absent [see Fig. 9(d)]. In the anomalous phase we directly get that  $I_{q,K} = -\infty$  by using the definition (65).

It has been shown in Ref. 23 that similar phenomenon can occur in the static multifractal spectrum  $f(\alpha)$  (related to generalized dimensions) of one-dimensional maps as well. It is worth noting furthermore, that examples have been found in other context which exhibit one-sided  $f(\alpha)$  multifractal spectra.<sup>99–102</sup> In particular, in fractal aggregates this property is caused by the extremely low growth probability inside the fjords.

A different mechanism leads to the existence of an anomalous phase in complete maps with infinitely many branches.<sup>103</sup> From the monotonicity properties of  $K(q)$  the

presence of this anomalous phase for  $q < 0$  is obvious since  $K(0) = \infty$  in such maps. The critical value  $q_c$  can, however, be now anywhere in the region  $0 \leq q_c \leq 1$  depending on the mixing properties of the branches.<sup>103</sup> As an example let us mention the Gauss map,<sup>104</sup> which also has relevance in cosmology describing the anisotropy fluctuations of the metric close to the cosmological singularity,<sup>105</sup> for which it was proven<sup>103</sup> that  $q_c = 1/2$ .

Finally a few general remarks are in order. In complete non-FDC maps modeling Lorenz-type systems both types of robust phase transitions can occur simultaneously.<sup>106</sup>

A sufficient condition for the phase transition can be formulated by generalizing the criterions given above. To this purpose let us consider the following bounds for the Rényi entropies<sup>107</sup>

$$K(q) \leq \frac{q}{q-1} \alpha \lambda, \quad q > 1, \quad (81)$$

$$K(q) \geq \frac{q}{q-1} \alpha \lambda, \quad q < 0, \quad (82)$$

where  $\alpha$  is the pointwise dimension<sup>5</sup> at any unstable periodic orbit, and  $\lambda$  is the Lyapunov exponent of the same orbit. We note that neither  $\alpha$  nor  $\lambda$  are invariant under coordinate changes,  $\alpha \lambda$  is, however, invariant just like  $K(q)$ . These relations lead to the unexpected result that intermittency is not necessarily connected with the existence of a marginally unstable periodic orbit, it might also be caused by an extremely strong feedback mechanism yielding a vanishing pointwise dimension around any of the periodic orbits with finite Lyapunov exponents.<sup>107</sup>

## V. OUTLOOK

In this paper we have restricted our attention to single humped 1D maps with complete symbolic dynamics, i.e., to cases when there was no exclusion rule for the grammar. That situation was found in entire intervals of generic control parameters in transiently chaotic cases reflecting the structural stability of the hyperbolic invariant set. Completeness holds on a more restricted space of control parameters in the case of permanent chaos.

A possible extension of the method includes parameter settings at which finite Markov partitions can be found. This means that certain symbol sequences are no longer allowed to occur, but the exclusion rules are of finite type. In such cases many of our results are expected to hold. One can define thermodynamics, generalized Frobenius–Perron equations, and show that their eigenvalues are connected with multifractal spectra exactly in the same manner as in the bulk of the paper. The computation is of course the more cumbersome the longer the grammatical rules are.

As for the most general case without any finite Markov partition, we hope that certain parameter values can be reached at least via a convergent series of parameter values at which Markov partitions of increasing length can be found.<sup>82</sup> In this way also thermodynamic functions can be obtained as limits of thermodynamic function computed at finite Markov partitions.

Certain aspects might go even beyond one dimension. The hierarchical organization of higher-dimensional chaos can be described by means of thermodynamical quantities. Instead of the cylinder set, it is worth taking in two-dimensional maps the intervals generated by intersecting the *stable manifold* with a smooth line. By measuring the scaling of the lengths of these intervals a free energy can be defined from which important characteristics connected with the expanding direction can be derived in hyperbolic cases.<sup>108</sup> One might also speculate about the applicability of the operator formalism to higher-dimensional maps. The operators and the derivatives appearing in them have to be defined then along the unstable manifolds. Because of the complicated fractal structure in the orthogonal directions, however, a practical computation seems to be rather cumbersome, but we think the problem deserves further attention.

One of the most general properties of chaos having played a role in the paper is the robustness of the Rényi entropies under coordinate transformations. In higher-dimensional cases they are also invariant against measure-preserving transformations which might also be singular, while the other characteristics are invariant under nonsingular coordinate changes only. The former, strong, invariance property also hold for the entropy decay or the entire spectrum of the corresponding transfer matrix. Another consequence of invariance is the rarity of phase transitions exhibited by entropies. The phase transitions characterize the dynamics at the border of chaos like at intermittency or super instability.

Bounds (81) and (82) for the entropies can easily be generalized<sup>107</sup> to higher-dimensional maps and time-continuous cases by simply replacing  $\alpha \lambda$  by  $\sum_j^+ \alpha_j \lambda_j$  where the sum is taken over different unstable directions, and  $\alpha_j$  and  $\lambda_j$  denote the pointwise dimension and the Lyapunov exponent of the unstable periodic orbit, respectively, taken along direction  $j$ .

In conclusion, a regular (anomalous) phase is present in  $K(q)$  for  $q > 1$  (for  $q < 0$ ) if either

(a) there exists a periodic orbit for which  $\sum_j^+ \alpha_j \lambda_j = 0$  ( $\sum_j^+ \alpha_j \lambda_j = \infty$ ) or

(b) there exist a series of periodic orbits for which  $\sum_j^+ \alpha_j \lambda_j$  can be arbitrarily close to zero (can be an arbitrarily large positive number). In continuous time dynamics possibility (a) occurs in the Lorenz attractor at the weak intermittent state.<sup>109</sup> In generic Hamiltonian systems where the phase space contains regular islands and chaotic regions there is a series of unstable periodic orbits approaching the boundary KAM tori for which  $\sum_j^+ \alpha_j \lambda_j$  can be arbitrarily small. Thus  $K(q) \equiv 0$  for  $q > 1$  for any generic Hamiltonian system.<sup>110</sup> This is a quantitative expression of the “sticking property” of KAM tori which property has recently been turned out to be essential in correctly interpreting an experiment on the magnetoresistance of mesoscopic two-dimensional conductors.<sup>111</sup>

It is worth recalling certain aspects that are also relevant beyond the scope of dynamical systems. The essence of these robust transitions in a *nonexponential scaling* in certain regions of the system. Such anomalous scaling

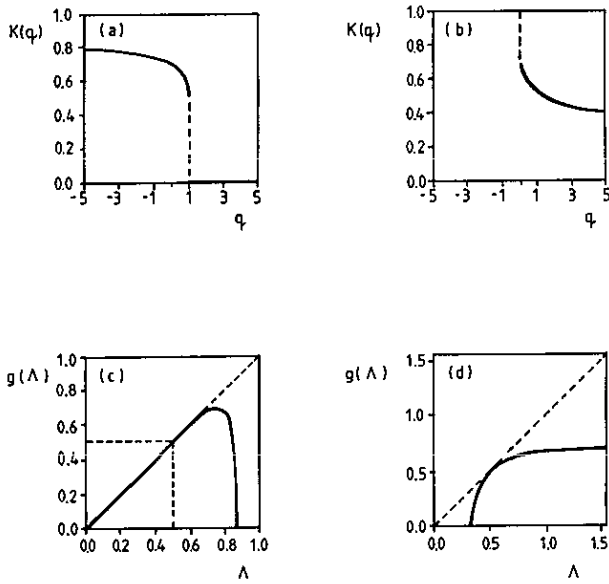


FIG. 9. Rényi entropies and dynamical multifractal spectra  $g(\Lambda)$  in borderline situations of chaos illustrated on the example of map (15). Intermittent case ( $d=1$ ); (a), (c); super unstable case  $d=-1$ ; (b), (d).

might occur in characteristics different from entropies, too. The intermittently transition of the entropies in self-organized critically<sup>98</sup> and the one-sided  $f(\alpha)$  of random resistor networks<sup>99</sup> and fractal aggregates<sup>17,101,102</sup> mentioned in the paper are notable examples.

Finally we remark that the universal chaos map, whose properties have been discussed throughout the paper, can also be relevant to higher-dimensional systems in the vicinity of the onset of chaos.

## ACKNOWLEDGMENTS

We are indebted for useful discussions and fruitful collaborations to members of our group on dynamical system: J. Bene, Á. Fülöp, Z. Kaufmann, Z. Kovács, K. G. Szabó, and G. Vattay.

This work has been supported by the National Scientific Research Foundation under the Grant Nos. OTKA 2090, F4489, and F4772.

## APPENDIX A: PERTURBATION THEORY

In what follows we will briefly review perturbation theory for the spectral properties of the Frobenius–Perron operator, a method which is applied to more general operators as well.

Suppose we have a perturbed map

$$f(\epsilon, x) = f_0(x) + \epsilon f_1(x), \quad (83)$$

where  $f_0$  is the zeroth-order map and  $f_1$  is the perturbation. It is assumed that they are piecewise analytic functions and the FDC property is maintained for  $f(\epsilon, x)$ . The spectral properties of  $\hat{H}_0$  associated with  $f_0$  are assumed to be known as

$$\lambda_{i,0} v_{i,0}(x) = \hat{H}_0 v_{i,0}(x), \quad (84)$$

where  $i$  labels the eigenvalues and eigenfunctions. Expand the operator  $\hat{H}(\epsilon)$  in terms of  $\epsilon$  like

$$\hat{H}(\epsilon) = \sum_{j=0}^{\infty} \hat{H}_j \epsilon^j. \quad (85)$$

The operator  $\hat{H}_j$  can be expressed in terms of  $f_0$  and  $f_1$ . The first-order one is, e.g., given for a symmetric map (83) by  $\hat{H}_1 v(x) = -(f_1(f_0^{-1}(x)) \hat{H}_0 v(x))'$ , where because of the symmetry of  $f_1(x)$  any branch of the inverse  $f_0^{-1}$  can be taken. A further assumption is that the eigenvalues  $\lambda_i(\epsilon)$  and eigenfunctions  $v_i(\epsilon, x)$  are analytic in  $\epsilon$

$$\lambda_i(\epsilon) = \sum_{j=0}^{\infty} \lambda_{i,j} \epsilon^j, \quad (86)$$

$$v_i(\epsilon, x) = \sum_{j=0}^{\infty} v_{i,j}(x) \epsilon^j. \quad (87)$$

Expand both sides of the eigenvalue problem (and omit the label  $i$  and the argument  $x$ )

$$\lambda(\epsilon) v(\epsilon) = \hat{H}(\epsilon) v(\epsilon) \quad (88)$$

and obtain in the  $j$ th order

$$(\lambda_0 - \hat{H}_0) v_j = \sum_{i=1}^j (\hat{H}_i - \lambda_i) v_{j-i}. \quad (89)$$

If  $\lambda_1, \dots, \lambda_{j-1}$  and  $v_1, \dots, v_{j-1}$  are known, then the  $j$ th correction to the eigenvalue  $\lambda_j$  can be determined from the condition that the right-hand side must not contain the zeroth-order eigenfunction  $v_0$  as a component, since that component is eliminated on the left-hand side. Note that since the Frobenius–Perron operator is not self-adjoint, the projection onto the eigenfunction  $v_0$  should be worked out specifically for a given zeroth-order map. Denote the projector to  $v_0$  by  $\hat{\Pi}_0$ , then

$$\lambda_j v_0 = \hat{\Pi}_0 \left( \hat{H}_j v_0 + \sum_{i=1}^{j-1} (\hat{H}_i - \lambda_i) v_{j-i} \right), \quad j > 1. \quad (90)$$

The sum is absent for  $j=1$ . Once  $\lambda_j$  is determined, we can calculate the corresponding correction to the eigenfunction as

$$v_j = (\lambda_0 - \hat{H}_0)^{-1} (1 - \hat{\Pi}_0) \left( \hat{H}_j v_0 + \sum_{i=1}^{j-1} (\hat{H}_i - \lambda_i) v_{j-i} \right). \quad (91)$$

Clearly one does not expect any correction to  $\lambda_0(\epsilon) = 1$ , and the invariant probability density is the corresponding normalized eigenfunction  $P(\epsilon, x) = v_0(\epsilon, x)$ .

It should be emphasized that the space of eigenfunctions does not typically span the whole function space of interest. In the general case, so called null functions<sup>112</sup> should be included in the treatment as well, which are specified by that they are transformed into zero after a finite number of applications of the operator  $\hat{H}$ . The problem of the interplay between eigenfunctions and null functions is beyond our scope. In the case of FDC maps and function space we are considering, apart from intermittent maps, at the top of the spectrum the levels are well defined

and there are finite distances between them and perturbation theory for the eigenfunctions can be applied.

In order to give a few examples, we will consider the tent map as zeroth-order map, with the known spectrum and eigenfunctions for  $\hat{H}_0$ , when the space of functions is restricted to analytic ones on  $I$ :

$$\lambda_{i,0}=4^{-i}, \quad \nu(x)_{i,0}=B_{2i}(x/2), \quad (92)$$

where  $B_n(x)$  is the Bernoulli polynomial of order  $n$ , and 0 is a degenerate eigenvalue with eigenfunctions odd with respect to  $1/2$ . The invariant density is  $B_0(x/2) \equiv 1$ . The projection on the  $i$ th eigenfunction goes as

$$\hat{\Pi}_{i,0}\phi(x)=\nu(x)_{i,0}\frac{4^i}{(2i)!}\int_I\frac{d^{2i}}{dy^{2i}}\phi(y)dy. \quad (93)$$

Here we show the example of the bilinear map

$$f_{BL}(\epsilon,x)=1-(1-\epsilon)|1-2x|-\epsilon(1-2x)^2. \quad (94)$$

Perturbation theory for  $f_{BL}$  leads to the eigenfunction with unit eigenvalue

$$P_{BL}(\epsilon,x)\approx 1+\epsilon(1-2x)+\epsilon^2(8x^2-10x+7/3)+\epsilon^3(84x^3-150x^2+80x-11)/3+\dots \quad (95)$$

The bilinear map is related to the tent map by combining conjugation (11) with the transverse transformation (14), so in higher orders the correction to the probability density is not of odd symmetry. The full spectrum is given in first order

$$\lambda_i(\epsilon)\approx 4^{-i}(1-\epsilon i(2i+1)+\dots), \quad (96)$$

while the next-to-leading eigenvalue is to  $O(\epsilon^3)$

$$\lambda_1(\epsilon)\approx 1/4(1-3\epsilon+4\epsilon^2-5\epsilon^3+\dots). \quad (97)$$

The framework outlined above can be applied to the generalized Frobenius–Perron operator  $\hat{H}_f(q)$  as well. As examples we give for the case of the piecewise parabolic map (15) to  $O(d^3)$  the generalized Rényi entropies

$$K(q)=\ln 2-\frac{qd^2}{6}-\frac{q(q-1)d^3}{9}+\dots \quad (98)$$

and the entropy decay rates

$$\gamma(q)=\min(\phi(q),\eta(q)), \quad q\neq 1 \quad (99)$$

with

$$\phi(q)=\ln 4-d(2q+1)+\frac{d^2}{2}(8q^2+10q+3)-\frac{d^3}{9}(4q^3+16q^2+16q+3)+\dots, \quad (100)$$

$$\eta(q)=\ln 4-\frac{d^2}{3}(2q+1)-\frac{2d^3}{9}(3q^2+2q+1)+\dots, \quad (101)$$

and for  $q=1$

$$\gamma(1)=\ln 4-d^2-\frac{4d^3}{3}+\dots \quad (102)$$

## APPENDIX B: RANDOM FIELD ISING CHAIN

One-dimensional maps often show up in the theory of disordered systems<sup>113–116</sup> and can be studied by means of the methods described in the paper. As an illustrative example, we consider here the case of the random field Ising chain.

Take a semi-infinite chain of Ising spins  $\{s_1, s_2, \dots, s_n, \dots\}$  in an inhomogeneous external field  $\{h_1, h_2, \dots, h_n, \dots\}$  with Hamiltonian

$$\frac{H}{k_B T}=\sum_{j=1}^{\infty}(Ks_j s_{j+1}+h_j s_j), \quad (103)$$

where  $K$  is a coupling constant. The set of local fields  $\{h_j\}$  is considered as a particular realization of a random field distribution assuming at each site the values  $+h$  and  $-h$  with probabilities  $p$  and  $1-p$ , respectively.

The thermal properties of the system are obtained by evaluating the partition sum

$$Z=\sum_{\{s_1, s_2, \dots\}} \exp\left(-Ks_1 s_2 - h_1 s_1 - \sum_{j=2}^{\infty}(Ks_j s_{j+1} + h_j s_j)\right) \quad (104)$$

at a fixed realization of the fields and averaging the free energy over different realizations afterwards. The summation over spins can be made in a recursive way.<sup>117</sup> Since the first spin appears in two terms of  $H$  only, the partial sum is easily obtained in the form

$$Z=\sum_{\{s_2, s_3, \dots\}} 2 \cosh(Ks_2 + h_1) \times \exp\left(-\sum_{j=2}^{\infty}(Ks_j s_{j+1} + h_j s_j)\right). \quad (105)$$

As  $s_2$  can take on the values  $\pm 1$  only, an exponential representation of the cosh function gives

$$\cosh(Ks_2 + h_1)=\exp(A(K, h_1) + g(K, h_1)s_2), \quad (106)$$

where

$$A(K, x)=\frac{1}{2}\ln(\cosh(K+x)\cosh(K-x)), \quad (107)$$

$$g(K, x)=\frac{1}{2}\ln(\cosh(K+x)/\cosh(K-x)).$$

This form shows that the first spin gives the contribution  $-A(K, h_1)$  to the free energy, and generates simultaneously also an extra field  $g(K, h_1)$  for the second spin. The partition sum can thus be written as

$$Z=\sum_{\{s_2, s_3, \dots\}} \exp(A(K, h_1)) \exp\left(-Ks_2 s_3 - x_2 s_2 - \sum_{j=3}^{\infty}(Ks_j s_{j+1} + h_j s_j)\right), \quad (108)$$

where  $x_2$  is an effective field acting on the second spin, and is given by

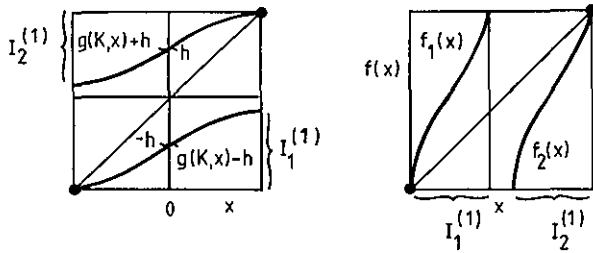


FIG. 10. Left: Random map generating the local field  $x$ . Right: The inverse of the map. The repeller of this map is the attractor of the random iteration (110) for any choice of the probability  $p$ .

$$x_2 = h_2 + g(K, h_1). \quad (109)$$

Note that the partition sum has a similar form to the original one (with  $x$  rather than  $h$  for the second spin). Hence, the summation over subsequent spins can be carried out in an analogous way. After  $n$  steps we find the field acting on spin  $(n+1)$  as

$$x_{n+1} = h_{n+1} + g(K, x_n) \quad (110)$$

and the actual contribution to the free energy will be  $-A(K, x_n)$ .

Thus, a recursion has been found which is actually a *random* one since the fields  $\{h_j\}$  are random variables.<sup>118</sup> According to the field distribution,  $x_{n+1}$  takes on the values  $h+g(K, x_n)$  and  $-h+g(K, x_n)$  with probability  $p$  and  $1-p$ , respectively. Consequently, the recursion can be written as a *two valued* map in which iterates stay on the upper [lower] branch with probability  $p[1-p]$  (see Fig. 10). The actual form of the map depends only on the coupling constant  $K$  and the field magnitude  $h$ . Although the branches alone are not expanding, the random map exhibits its chaotic motion on an attractor. The natural invariant measure on this attractor is of great importance since the averaged thermal free energy per spin is just the mean value of  $-A(K, x)$  taken with respect to the natural measure of variable  $x$  on the attractor. The averaged magnetization per spin and other thermal properties can also be expressed by means of the natural measure.<sup>118</sup>

At certain parameter settings there is a gap between the branches as shown on Fig. 10. This has the consequence that the attractor is a *fractal*. One sees immediately that the whole interval  $I$  on which the dynamics is defined is mapped then into two smaller ones with the gap in between, and the images of the small intervals will have also holes, in any order. In fact, these intervals are exactly the *cylinders* in the *inverted* map shown on the right of Fig. 10. Thus, one concludes that the attractor of the random map is just the *repeller* of the inverted map.<sup>119</sup> This statement holds for all values of probability  $p$ . The natural measure on the attractor, however, depends strongly on the choice of  $p$  and is not related to the natural measure of the repeller.

The natural measure of the attractor of the random map can, of course, be obtained by iterating the map  $f$  (see Fig. 10) backward with branching probabilities  $p$  and  $1-p$ , and is independent of the choice of the initial point.

The measure is a multifractal measure.<sup>120,121</sup> An efficient way to obtain its  $D(q)$  spectrum is to solve the eigenvalue equation (45) with  $p_1(x) = 1-p, p_2(x) = p$ . In numerical solutions, one adjusts the exponent of the denominator such that the iteration converges towards a finite limiting function from which the value of  $D(q)$  follows. Alternatively, a perturbation expansion can also be worked out. In the limit of small magnetic fields  $h$  one finds<sup>65,121</sup>

$$D(q) = \frac{1}{q-1} \ln [p^q + (1-p)^q] \frac{1}{\ln v} \left( 1 + \frac{1}{\ln v} \right. \\ \left. \times \left( 1 + \frac{2v}{1-v} \left( \frac{1}{k_B T} \right)^2 \right) h^2 + G(v, q, T) h^4 + \dots \right), \quad (111)$$

where  $v = \tanh K$  and  $G$  denotes a complicated function not given here explicitly. Note that while the auxiliary variable  $x$  has a monofractal structure for small  $h$  and  $p = 1/2$ , the local magnetization develops multiscaling behavior even in that region.<sup>122</sup>

It is interesting to note that free energy fluctuations which are due to different realizations of the random field in finite chains are closely related to the multifractal spectrum of the natural measure,<sup>121</sup> and similar results can be obtained if magnetic field is not present but the coupling constant  $K$  is randomly distributed along the chain.<sup>123</sup>

<sup>1</sup> P. Cvitanović, *Universality in Chaos* (A. Hilger, Bristol, 1984).

<sup>2</sup> Hao Bai-lin, *Chaos* (World Scientific, Singapore, 1984).

<sup>3</sup> P. Collet, J.-P. Eckmann, *Iterated Maps of the Interval as Dynamical Systems* (Birkhäuser, Basel, Boston, 1980).

<sup>4</sup> H. G. E. Hentschel and I. Procaccia, *Physica D* **8**, 435 (1983); P. Grassberger, *Phys. Lett. A* **97**, 227 (1983).

<sup>5</sup> T. C. Halsey *et al.*, *Phys. Rev. A* **33**, 1141 (1986).

<sup>6</sup> J. P. Eckmann and I. Procaccia, *Phys. Rev. A* **34**, 659 (1986).

<sup>7</sup> A. Rényi, *Probability Theory* (North-Holland, Amsterdam, 1970).

<sup>8</sup> P. Grassberger and I. Procaccia, *Phys. Rev. A* **28**, 2591 (1983).

<sup>9</sup> H. Fujisaka, *Prog. Theor. Phys.* **70**, 1264 (1983); **71**, 513 (1984).

<sup>10</sup> R. Benzi, G. Paladin, G. Parisi, and A. Vulpiani, *J. Phys. A* **18**, 2157 (1985); P. Grassberger, in *Chaos*, edited by A. V. Holden (Manchester University, Manchester, 1986).

<sup>11</sup> Y. G. Sinai, *Usp. Mat. Nauk.* **27**, 21 (1972). [*Russ. Math. Surveys* **166**, 21 (1972)].

<sup>12</sup> R. Bowen, *Lect. Notes in Math.* **470**, 1 (1975).

<sup>13</sup> D. Ruelle, *Thermodynamic Formalism* (Addison-Wesley, Reading, 1978).

<sup>14</sup> H. Mori, H. Hata, T. Horita, and T. Kobayashi, *Progr. Theor. Phys.* **99**, 1 (1989).

<sup>15</sup> T. Yoshida and S. Miyazaki, *Progr. Theor. Phys.* **99**, 64 (1989).

<sup>16</sup> H. Fujisaka and M. Inoue, *Progr. Theor. Phys.* **99**, 82 (1989).

<sup>17</sup> T. Bohr and T. Tél, in *Direction in Chaos*, edited by U. Bai-lin Hao (World Scientific, Singapore, 1988).

<sup>18</sup> R. Badii, *Riv. Nuovo Cim.* **12**, 1 (1989).

<sup>19</sup> P. Grassberger, R. Badii, and A. Politi, *J. Stat. Phys.* **51**, 135 (1988).

<sup>20</sup> P. Szépfalussy and T. Tél, *Phys. Rev. A* **35**, 477 (1987).

<sup>21</sup> P. Szépfalussy, T. Tél, A. Csordás, and Z. Kovács, *Phys. Rev. A* **36**, 3525 (1987).

<sup>22</sup> A. Csordás, and P. Szépfalussy, *Phys. Rev. A* **38**, 2582 (1988).

<sup>23</sup> A. Csordás, and P. Szépfalussy, *Phys. Rev. A* **39**, 4767 (1989).

<sup>24</sup> T. Tél, in *Directions in Chaos, Vol. 3*, edited by Hao Bai-lin (World Scientific, 1990), pp. 149–211.

<sup>25</sup> R. Artuso, E. Aurell, and P. Cvitanović, *Nonlinearity* **3**, 325, 361 (1990).

<sup>26</sup> P. Szépfalussy and T. Tél, *Phys. Rev. A* **34**, 2520 (1986).

<sup>27</sup> T. Tél, *Phys. Rev. A* **36**, 2507 (1987).

<sup>28</sup> H. Fujisaka and M. Inoue, *Prog. Theor. Phys.* **78**, 268 (1987).

<sup>29</sup> M. Misiurewicz, *Publ. Math. IHES* **53**, 17 (1981).

- <sup>30</sup>C. Grebogi, E. Ott, and J. A. Yorke, *Phys. Rev. Lett.* **48**, 1507 (1982); *Physica D* **7**, 181 (1983).
- <sup>31</sup>S.-J. Chang and I. Wright, *Phys. Rev. A* **23**, 1419 (1981); H. Daido, *Prog. Theor. Phys.* **67**, 1698 (1982).
- <sup>32</sup>G. Györgyi and P. Szépfalussy, *J. Stat. Phys.* **34**, 45 (1984).
- <sup>33</sup>S. Grossmann and S. Thomae, *Z. Naturforsch.* **32a**, 1358 (1977).
- <sup>34</sup>G. Györgyi and P. Szépfalussy, *Z. Phys. B* **55**, 179 (1984).
- <sup>35</sup>P. Szépfalussy, in *Proceedings of the Conference on Synergetics, Order and Chaos, Madrid, 1987*, edited by M. Velarde (World Scientific, Singapore, 1988).
- <sup>36</sup>S. Grossmann and H. Horner, *Z. Phys. B* **60**, 79 (1985).
- <sup>37</sup>G. Györgyi and P. Szépfalussy, *Acta Phys. Hung.* **64**, 34 (1988).
- <sup>38</sup>V. M. Alekseev and M. V. Jakobson, *Phys. Rep.* **75**, 290 (1980).
- <sup>39</sup>A. Kolmogorov, *Dokl. Akad. Nauk. SSSR* **119**, 861 (1958).
- <sup>40</sup>Ya. G. Sinai, *Dokl. Akad. Nauk. SSSR* **124**, 768 (1959).
- <sup>41</sup>J. P. Eckmann and D. Ruelle, *Rev. Mod. Phys.* **75**, 617 (1985).
- <sup>42</sup>G. Györgyi and P. Szépfalussy, *Phys. Rev. A* **31**, 3477 (1985).
- <sup>43</sup>P. Szépfalussy and G. Györgyi, *Phys. Rev. A* **33**, 2852 (1986).
- <sup>44</sup>R. Kluiving, H. W. Capel, and R. A. Pasmanter, *Physica A* **183**, 67 (1992); **183**, 96 (1992).
- <sup>45</sup>M. Misiurewicz and K. Ziemian, "Rate of convergence for computing entropy of some one-dimensional maps," Preprint.
- <sup>46</sup>P. Szépfalussy, *Phys. Scrip.* **T25**, 226 (1989).
- <sup>47</sup>P. Grassberger, *Int. J. Theor. Phys.* **25**, 907 (1986).
- <sup>48</sup>J. Bene and P. Szépfalussy, *Phys. Rev. A* **37**, 871 (1988).
- <sup>49</sup>F. Christiansen, G. Paladin, and H. H. Rugh, *Phys. Rev. Lett.* **62**, 2087 (1990).
- <sup>50</sup>R. W. Rollins and E. R. Hunt, *Phys. Rev. A* **29**, 3327 (1984).
- <sup>51</sup>L. P. Kadanoff and C. Tang, *Proc. Natl. Acad. Sci. USA* **81**, 12 (1984).
- <sup>52</sup>H. Kantz and P. Grassberger, *Physica D* **17**, 75 (1985).
- <sup>53</sup>D. Ruelle, *Ergod. Th. Dynam. Syst.* **2**, 99 (1982).
- <sup>54</sup>H. McCluskey and A. Manning, *Ergod. Th. Dynam. Syst.* **3**, 251 (1983).
- <sup>55</sup>K. J. Falconer, *J. Phys. A* **21** L737 (1988).
- <sup>56</sup>T. Bohr and D. Rand, *Physica D* **25**, 387 (1987).
- <sup>57</sup>G. Pianigiani and J. A. Yorke, *Trans. Am. Math. Soc.* **252**, 351 (1979); G. Pianigiani, *J. Math. Anal. Appl.* **82**, 75 (1981).
- <sup>58</sup>A. Csordás, thesis, Budapest, 1989 (in Hungarian).
- <sup>59</sup>T. Tél, *Phys. Rev. A* **36**, 1502 (1987).
- <sup>60</sup>E. Ott, T. Sauer, and J. A. Yorke, *Phys. Rev. A* **39**, 4212 (1989).
- <sup>61</sup>T. Tél, *J. Phys. A* **22**, L691 (1989).
- <sup>62</sup>Z. Kovács and T. Tél, *Phys. Rev. A* **45**, 2270 (1992).
- <sup>63</sup>T. Tél, *Phys. Lett. A* **119**, 65 (1986).
- <sup>64</sup>S. Vienti, *J. Phys. A* **21**, 2023, 2313 (1988).
- <sup>65</sup>J. Bene, *Phys. Rev. A* **39**, 2090 (1989).
- <sup>66</sup>M. J. Feigenbaum, *J. Stat. Phys.* **52**, 527 (1988).
- <sup>67</sup>Z. Kovács, *J. Phys. A* **22**, 5161 (1989).
- <sup>68</sup>F. Christiansen, P. Cvitanović, and H. H. Rugh, *J. Phys. A* **23**, L713 (1990).
- <sup>69</sup>P. Walters, *Am. J. Math.* **97**, 937 (1975).
- <sup>70</sup>D. H. Mayer, *Lect. Notes in Phys.* **123**, 1 (1980).
- <sup>71</sup>G. Keller, *Commun. Math. Phys.* **96**, 181 (1984); D. Ruelle, *Phys. Rev. Lett.* **56**, 465 (1986); D. Ruelle, *J. Stat. Phys.* **44**, 281 (1986).
- <sup>72</sup>D. H. Mayer, *Phys. Lett. A* **121**, 390 (1987); D. H. Mayer and G. Roepstorff, *J. Stat. Phys.* **47**, 149 (1987).
- <sup>73</sup>P. Collet, J. Lebowitz, and A. Porzio, *J. Stat. Phys.* **47**, 609 (1987); A. Arneodo and M. Holschneider, *ibid.* **50**, 995 (1988); D. Bessis et al. *ibid.* **51**, 109 (1988).
- <sup>74</sup>V. Baladi, J. P. Eckmann, and D. Ruelle, *Nonlinearity* **2**, 119 (1989); A. O. Lopes, *SIAM J. Math. Anal.* **20**, 1243 (1989).
- <sup>75</sup>M. Sano, S. Sato, and M. Sawada, *Prog. Theor. Phys.* **76**, 945 (1986).
- <sup>76</sup>M. J. Feigenbaum, M. H. Jensen, and I. Procaccia, *Phys. Rev. Lett.* **56**, 1503 (1986).
- <sup>77</sup>M. H. Jensen, L. P. Kadanoff, and I. Procaccia, *Phys. Rev. A* **36**, 1409 (1987).
- <sup>78</sup>M. J. Feigenbaum, *J. Stat. Phys.* **46**, 919, 925 (1987).
- <sup>79</sup>M. Kohmoto, *Phys. Rev. A* **37**, 1345 (1987).
- <sup>80</sup>P. Cvitanović, in *Nonlinear Physical Phenomena*, edited by A. Ferraz et al. (World Scientific, Singapore, 1990).
- <sup>81</sup>C. Beck, *Physica D* **50**, 1 (1991); W. Just, *J. Stat. Phys.* **67**, 271 (1992).
- <sup>82</sup>M. J. Feigenbaum, I. Procaccia, and T. Tél, *Phys. Rev. A* **39**, 5359 (1989).
- <sup>83</sup>I. Procaccia and R. Zeitak, *Phys. Rev. Lett.* **50**, 2511 (1988).
- <sup>84</sup>H. Mori et al., *Prog. Theor. Phys.* **81**, 60 (1989).
- <sup>85</sup>T. Kobayashi et al., *Prog. Theor. Phys.* **82**, 1 (1989).
- <sup>86</sup>H. Fujisaka and H. Shibata, *Prog. Theor. Phys.* **85**, 187 (1991).
- <sup>87</sup>T. Prellberg and J. Slawny, *J. Stat. Phys.* **60**, 503 (1992).
- <sup>88</sup>X. J. Wang, *Phys. Rev. A* **40**, 6647 (1989); H. Fujisaka and M. Inoue, *ibid.* **41**, 5302 (1990); A. Porzio, *J. Stat. Phys.* **58**, 923 (1990).
- <sup>89</sup>R. Stoop et al., *Z. Naturforsch.* **46a**, 642 (1991); R. Stoop and J. Parisi, *Phys. Rev. A* **43**, 1802 (1991); R. Stoop et al., *Physica D* **50**, 405 (1991).
- <sup>90</sup>H. Shigematsu, *J. Stat. Phys.* **66**, 727 (1992); W. Just and H. Fujisaka, *J. Phys. A* **25**, 3567 (1992).
- <sup>91</sup>G. Paladin, L. Peliti, and A. Vulpiani, *J. Phys. A* **19**, L991 (1986).
- <sup>92</sup>H. Fujisaka and M. Inoue, *Prog. Theor. Phys.* **77**, 1334 (1987).
- <sup>93</sup>P. Gaspard and X. J. Wang, *Proc. Natl. Acad. Sci. U.S.A.* **85**, 4591 (1988).
- <sup>94</sup>X. J. Wang, *Phys. Rev. A* **39**, 3214 (1989).
- <sup>95</sup>S. Sato and K. Honda, *Phys. Rev. A* **42**, 3233 (1990).
- <sup>96</sup>K. Honda and H. Kodama, *Phys. Lett. A* **149**, 101 (1990).
- <sup>97</sup>K. Honda, S. Sato, and H. Kodama, *Phys. Rev. A* **43**, 2669 (1991).
- <sup>98</sup>A. Erzan and S. Sinha, *Phys. Rev. Lett.* **66**, 2750 (1991); and (private communication).
- <sup>99</sup>G. G. Batrouni, A. Hansen, and S. Roux, *Phys. Rev. A* **38**, 3820 (1988).
- <sup>100</sup>T. Bohr, P. Cvitanović and M. H. Jensen, *Europhys. Lett.* **6**, 445 (1988).
- <sup>101</sup>J. Lee, S. Havlin, H. E. Stanley, and J. E. Kiefer, *Phys. Rev. A* **42**, 4832 (1990).
- <sup>102</sup>B. B. Mandelbrot, C. J. G. Evertsz, and Y. Hayakawa, *Phys. Rev. A* **42**, 4528 (1990).
- <sup>103</sup>A. Csordás and P. Szépfalussy, *Phys. Rev. A* **40**, 2221 (1989).
- <sup>104</sup>D. H. Mayer, *Commun. Math. Phys.* **130**, 311 (1990).
- <sup>105</sup>L. D. Landau and E. M. Lifschitz, *The Classical Theory of Fields*, 4th ed. (Pergamon, Oxford, 1975).
- <sup>106</sup>P. Szépfalussy, T. Tél, and G. Vattay, *Phys. Rev. A* **43**, 681 (1991).
- <sup>107</sup>J. Bene and P. Szépfalussy, *Phys. Rev. A* **46**, 801 (1992).
- <sup>108</sup>Z. Kovács and T. Tél, *Phys. Rev. Lett.* **64**, 1617 (1990).
- <sup>109</sup>Z. Kaufmann and P. Szépfalussy, *Phys. Rev. A* **40**, 2615 (1989).
- <sup>110</sup>J. Bene, P. Szépfalussy, and A. Fülöp, *Phys. Rev. A* **40**, 6719 (1989).
- <sup>111</sup>D. Weiss et al., *Phys. Rev. Lett.* **66**, 2790 (1991); R. Fleischmann, T. Geisel, and R. Ketzmerick, Preprint, 1991.
- <sup>112</sup>M. Dörfle, *J. Stat. Phys.* **40**, 93 (1985).
- <sup>113</sup>R. Rammal and G. Toulouse, *J. Physique Lett.* **44**, L13 (1983); R. Rammal, *J. Physique* **45**, 191 (1984).
- <sup>114</sup>M. Kohmoto, L. P. Kadanoff, and C. Tang, *Phys. Rev. Lett.* **50**, 1870 (1983).
- <sup>115</sup>M. Kohmoto and Y. Oono, *Phys. Lett. A* **102**, 145 (1984); J. Kollár and A. Sütö, *Phys. Lett. A* **117**, 203 (1986).
- <sup>116</sup>C. Van den Broeck, *Phys. Rev. A* **40**, 7334 (1989); C. Van den Broeck and V. Balakrishnan, *Ber. Bunsenges. Phys. Chem.* **95**, 342 (1991).
- <sup>117</sup>P. Ruján, *Physica A* **91**, 549 (1978).
- <sup>118</sup>G. Györgyi and P. Ruján, *J. Phys. C* **17**, 4207 (1984).
- <sup>119</sup>P. Szépfalussy and U. Behn, *Z. Phys. B* **65**, 337 (1987).
- <sup>120</sup>S. N. Evangelou, *J. Phys. C* **20**, L511 (1987).
- <sup>121</sup>J. Bene and P. Szépfalussy, *Phys. Rev. A* **37**, 1703 (1988).
- <sup>122</sup>G. Györgyi and I. I. Satija, *Phys. Rev. Lett.* **62**, 446 (1989).
- <sup>123</sup>T. Tanaka, H. Fujisaka, and M. Inoue, *Phys. Rev. A* **39**, 3170 (1989).